

Check for updates



The Diversity of the DNA-Binding Landscape in the DREB/ERF Family: Focusing on Reproductive Processes in Fruit Trees With Highly Heterozygous Genome

Fengqi $Wu^1 \mid Jiakun Zheng^1 \mid Huimin Hu^1 \mid Hongsen Liu^1 \mid Yaxuan Xiao^1 \mid Junting Feng^{2,3} \mid Yanwei Hao^1 \mid Chengjie Chen^{2,3} \mid Rui Xia^{1} \bigcirc \mid Zaohai Zeng^{1} \bigcirc$

¹State Key Laboratory for Conservation and Utilization of Subtropical Agro-Bioresources, Guangdong Laboratory for Lingnan Modern Agriculture, Key Laboratory of Biology and Genetic Improvement of Horticultural Crops (South China), Ministry of Agriculture and Rural Affairs, Guangdong litchi Engineering Research Center, College of Horticulture, South China Agricultural University, Guangzhou, China | ²State Key Laboratory of Tropical Crop Breeding, Key Laboratory of Crop Gene Resources and Germplasm Enhancement in South China, Ministry of Agriculture and Rural Affairs, Key Laboratory of Tropical Crops Germplasm Resources Genetic Improvement and Innovation of Hainan Province, Tropical Crops Genetic Resources Institute, Chinese Academy of Tropical Agricultural Sciences, Haikou, China | ³State Key Laboratory of Tropical Crop Breeding, Sanya Research Institute, Institute of Tropical Bioscience and Biotechnology, Chinese Academy of Tropical Agricultural Sciences, Haikou, China

Correspondence: Chengjie Chen (ccj@catas.cn) | Rui Xia (rxia@scau.edu.cn) | Zaohai Zeng (zengzh@scau.edu.cn)

Received: 18 February 2025 | Revised: 8 September 2025 | Accepted: 9 September 2025

Funding: This work was supported by the Key Area Research and Development Program of Guangdong Province, 2022B0202070003; National Natural Science Foundation of China, 32072547, 32102320, 32372665; the Project of State Key Laboratory of Tropical Crop Breeding, SKLTCBZRJJ202502.

Keywords: DAP-seq | DREB/ERF | lychee | maturation period | terpenoids

ABSTRACT

DREB/ERF transcription factors play pivotal roles in plant development; however, their structural characteristics, DNA-binding preferences, and functional roles in highly heterozygous woody plants remain insufficiently understood. Using lychee (*Litchi chinensis*) as a model, we identified 95 DREB/ERF genes subdivided into ten phylogenetic groups. DNA affinity purification sequencing (DAP-seq) of 45 representative members uncovered 65 194 binding sites with subfamily-specific motifs: C(G/A) CCG(A/C)C for DREB and CGCCG(C/T)C for ERF subfamilies. Each group exhibited unique binding motif preferences, aligning with their protein structures and essential peptide positions. Notably, LITCHI017494 directly regulated terpenoid biosynthesis and aroma formation by activating tandemly repeated LcTPS genes. Furthermore, single nucleotide polymorphisms (SNPs) in LITCHI017494's binding sites altered the binding efficiency of two flowering-related genes (*LcSVP* and *LcVOZ*) in early- and late-maturing haplotypes, revealing a mechanism underlying flowering and fruit maturation period. Overall, with experimental evidence, this study provides a comprehensive binding profile of the DREB/ERF family in lychee, revealing intricate transcriptional regulatory networks and serving as a crucial resource for transcription factor research within complex genomic contexts, especially in the DREB/ERF gene family.

1 | Introduction

Transcription factors (TFs) are proteins that bind to DNA in a sequence-specific manner, comprising more than 5% of the total genes in plant genomes. They are typically organised into large superfamilies, with each member serving a specific regulatory role, playing a critical role in regulating transcription (Riechmann and Ratcliffe 2000). Among these, the ethyleneresponsive factor (ERF) family has garnered significant attention due to its pivotal roles in various biological processes (Feng et al. 2020). The ERF family, belonging to the largest plant-specific TF families, AP2/EREBP superfamily, comprises two

This is an open access article under the terms of the Creative Commons Attribution-NonCommercial-NoDerivs License, which permits use and distribution in any medium, provided the original work is properly cited, the use is non-commercial and no modifications or adaptations are made.

© 2025 The Author(s). Plant Biotechnology Journal published by Society for Experimental Biology and The Association of Applied Biologists and John Wiley & Sons Ltd

main subfamilies: the DREB (Dehydration Responsive Element Binding protein) and ERF subfamilies (Han et al. 2022). From a phylogenetic perspective, the ERF family can be further subdivided into either 10 groups (DREB groups I-IV and ERF groups V-X) or 12 groups (DREB groups A-1 to A-6 and ERF groups B-1 to B-6) (Nakano et al. 2006; Sakuma et al. 2002). Members of the DREB and ERF subfamilies recognise similar but slightly different sequences (Yamasaki et al. 2013). Mostly, ERF transcription factors bind to the typical GCC-box element (5'-AGCCGCC-3') as well as a related, distinct GC-rich element (Shoji et al. 2013), while DREB transcription factors specifically bind the DRE ciselement (5'-A/GCCGAC-3') and a similar DRE (Dehydration Responsive Element) element, the C-repeat (TGGCCGAC) (Sakuma et al. 2002). Additionally, within the same subfamily, transcription factors can also exhibit distinct binding preferences. For example, OsDREB1C favours the GCCGAC motif, while AtCBF1/2/3 preferentially bind to A/GCCGAC (Deng et al. 2024). It is reported that a small number of amino acid residues in the DNA-binding domain are key determinants of these distinct binding specificities (Kagaya et al. 1999). In the AP2 domain of the DREB protein, the 14th and 19th amino acids are valine (V) and glutamate (E), whereas in the ERF protein, these positions are occupied by alanine (A) and aspartic acid (D). This difference influences the protein's ability to interact with the DRE or GCC box, thereby affecting the regulation of downstream target genes during transcription. This variation also suggests that members of the ERF and DREB subfamilies may participate in distinct regulatory pathways (Zhang et al. 2022). However, the precise mechanism by which these two proteins accurately recognise similar yet distinct DNA binding sites and regulate gene expression within different signal transduction pathways remains to be elucidated.

ERF/DREB transcription factors regulate a wide array of genes involved in stress responses, plant growth, and development (Rehman and Mahmood 2015). In wheat, the ERF gene TaSRL1 inhibits root growth through an auxin-dependent pathway by interacting with TaTIFY9 to integrate auxin and jasmonic acid signals (Zhuang et al. 2021). Moreover, ERFs have also been reported to regulate flowering time (Chen, Zhang, et al. 2021; Huang et al. 2022; Upadhyay et al. 2013), as well as fruit development (Durán-Medina et al. 2017; Yuste-Lisbona et al. 2020). ERF1, a key player in the ethylene signal transduction pathway, negatively influences flowering time by repressing FT transcription in Arabidopsis (Chen, Zhang, et al. 2021). Another member of group VIII, ENO (excessive number of floral organs), modulates floral meristem size by adjusting WUS expression in the CLV-WUS signalling cascade, thus influencing fruit size (Yuste-Lisbona et al. 2020). Additionally, ERFs have been implicated in governing the production of secondary metabolites, including anthocyanins, carotenoids, and capsaicin (Song, Liu, et al. 2023; Sun et al. 2024; Zhang, Yu, et al. 2024). CaERF102 and CaERF111 mutually regulate each other's transcription, impacting capsaicin biosynthesis directly or indirectly (Song, Liu, et al. 2023).

While extensive research has been conducted on ERFs, only one comprehensive global-scale profiling of binding site patterns for ERFs in the plant has been conducted, specifically in the model plant *Arabidopsis* (O'Malley et al. 2016). Furthermore, the model plant *Arabidopsis* exhibits a restricted range of reproductive

biological processes compared to long-lived woody species with perennial flowering cycles and intricate phenological patterns, including complex fleshy fruit development processes. As a consequence, fundamental aspects of DREB/ERF-mediated reproductive regulation remain undiscovered. Additionally, transcription factor binding sites are frequently influenced by single nucleotide polymorphisms (SNPs), and in highly heterozygous woody plants, haplotype-specific SNP variations may directly modify binding efficiency, introducing supplementary regulatory layers that are not observable in genetically homogeneous, inbred *Arabidopsis* lines.

Lychee (Litchi chinensis Sonn.) is a valuable perennial fruit tree native to Southeast Asia, bearing fresh fruit every summer, renowned for its rich nutritional content (Hu, Feng, et al. 2022). Our previous research has demonstrated that lychee possesses a highly heterozygous genome characterised by the presence of two major haplotypes: one associated with early flowering and the other with late flowering. This genetic diversity positions lychee as an ideal material for exploring the transcriptional regulatory mechanisms underlying the development of complex reproductive organs, particularly in species with intricate genomes. Furthermore, a comprehensive investigation into the molecular pathways governing lychee growth and development could provide valuable theoretical support for breeding new lychee varieties with desirable economic traits. Recent studies have also highlighted the significant role of ERF/DREB transcription factors in regulating processes such as flowering and fruit development and coloration, emphasising the need to identify and characterise the transcriptional regulatory roles and biological functions of these factors in this species (He et al. 2023; Zhuo et al. 2024).

In this study, 95 ERF/DREB family members were identified, and genome-wide DNA binding site maps were generated in vitro through DAP-seq for 45 lychee DREB/ERF transcription factors, representing all ten clades. Further analysis of the key gene LITCHI017494 uncovered its role in regulating terpenoid synthesis in lychee fruit, shedding light on potential regulatory mechanisms of ERF/DREB transcription factors in the lychee fruit maturation period. Also, an interesting regulatory relationship was found between binding site preference (contributed by two SNPs in two genes) of haplotypes and flowering time. These findings not only established a comprehensive database of potential binding sites and target genes of lychee ERF transcription factors but also served as a crucial step toward understanding their physiological roles and the regulatory mechanisms they mediate. Furthermore, this research will lay a solid foundation for future studies, offering candidate genes for molecularassisted breeding.

2 | Results

2.1 | Comparative Analysis of Sequence and Structure of DREB/ERF Transcription Factors in Lychee

DREB/ERF transcription factors play crucial roles in plant development, especially reproductive processes. Lychee (*Litchi chinensis*) is a valuable perennial fruit tree in southern China,

bearing fresh fruit with rich nutritional content (Hu, Feng, et al. 2022). Here, we use lychee as a model organism to investigate the binding site preferences and functions of the DREB/ERF gene family. A total of 95 members with complete protein-coding sequences were identified through homologous gene comparison and manual gene structure annotation review (Figure 1a, Table S1). Phylogenetic analysis grouped the DREB/ERF gene family into two primary subfamilies, DREB and ERF, which were further classified into 10 distinct groups. The DREB subfamily consists of 39 members categorised into 4 groups, while the ERF subfamily includes 56 members, organised into 6 groups. Protein domain analysis revealed that all DREB/ERF family members contain a single AP2 domain (Figure 1b, Figure S1a-c). All DREB proteins contain valine (V) at the aligned position 15 and a variable amino acid at position 20, with 23 of them being glutamic acid (E), which is an important characteristic of DREB proteins (Sakuma et al. 2002; Wu et al. 2022). In contrast, all ERF proteins possess conserved alanine (A) and aspartic acid (D) at the corresponding positions, except for group V, which, like the DREBs, contains valine (V) at position 15 and a variable amino acid at position 20 (Figure S1a-c). Additionally, protein folding predictions indicate that DREB members possess a core structure with two α -helixes and three β -sheets, whereas ERF members (excluding group V) display a core structure with one α -helix and three β -sheets. The rest of the structural elements, such as α-helixes, show considerable variability (Figure 1c, Figure S1b-d). These sequence and structural differences suggest that DREB and ERF subfamilies may exhibit varied DNA-binding characteristics and potentially divergent biological regulatory functions. Homology-based gene functional annotation indicates that lychee DREB/ERF genes may regulate the reported biological processes (supported by literature review) which include stress responses, growth and development, metabolism, and plant hormone signalling. Moreover, these regulatory functions appear to vary across different groups (Figure 1d).

2.2 | Binding Site Preferences of DREB/ERF Transcription Factors in Lychee

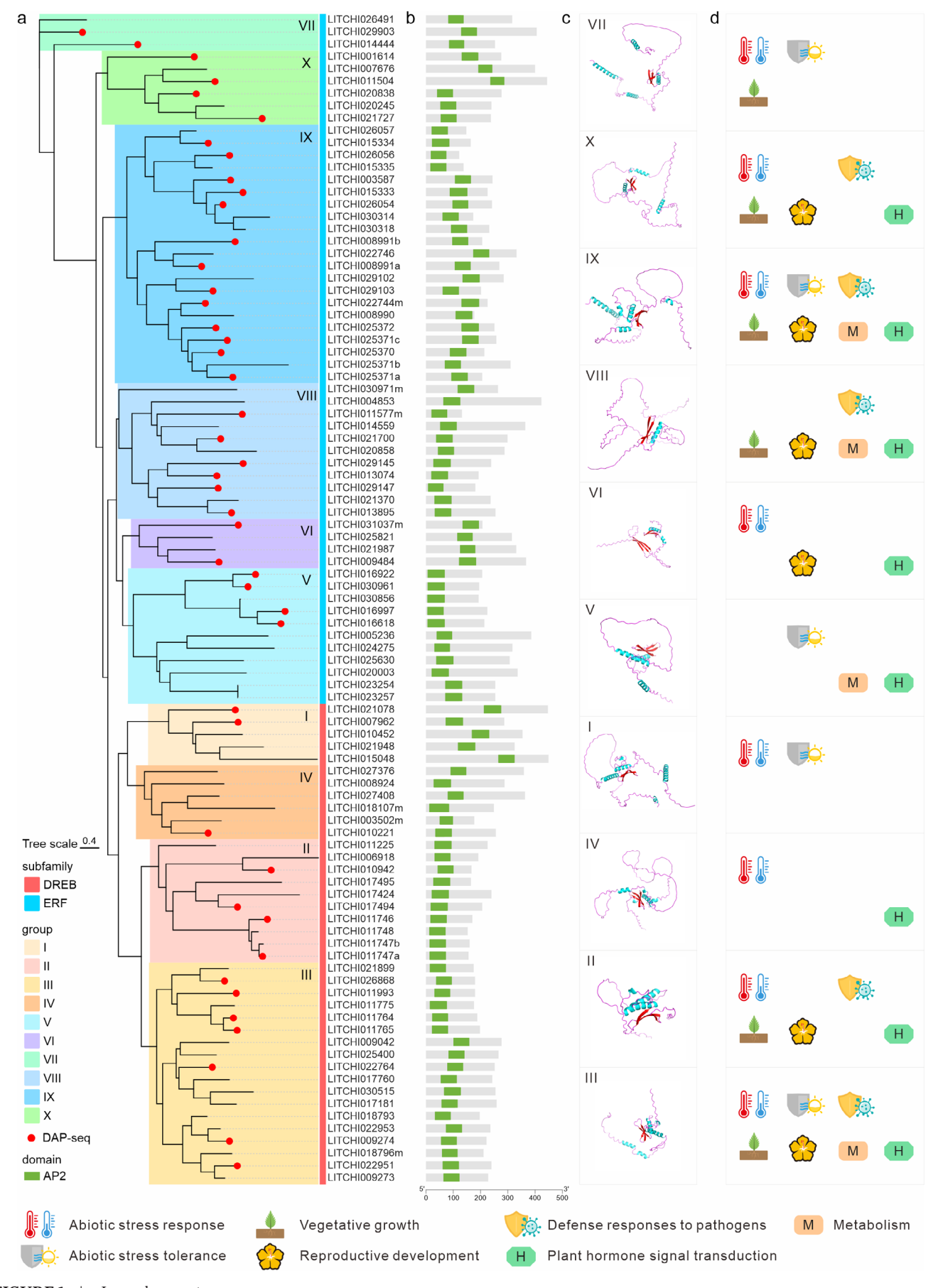
Do these sequence and structural differences in the DREB/ ERFs family groups affect their transcriptional regulatory functions? To address this question, DAP-seq libraries were successfully constructed and sequenced for 45 representative members of the lychee DREB/ERF family, selected for their phylogenetic diversity and expression profiles (Figure S2). Among these, 14 members were from the DREB subfamily and 31 from the ERF subfamily, with at least one member from each group, as shown in Figure 1a. The DREB/ERF gene family demonstrated a strong DNA-binding capability, with a total of 65194 binding sites identified, including 698 core peaks shared by the 45 sequenced members (Figure 2a). The DNAbinding abilities of the DREB and ERF subfamilies were comparable, with binding at 42 748 and 46 701 sites, respectively. The number of core binding sites was 1199 for DREB and 1180 for ERF (Figure 2a). The number of identified binding sites varied significantly across groups, ranging from 3309 to 39041. Groups IX, II, and I exhibited the strongest DNA-binding abilities (Figure 2b, Figure S3). The relatively low number of core binding sites suggested considerable variability in DNA-binding sites among different DREB/ERF members. Analysis revealed that the two major subfamilies primarily bind to gene exons and intergenic regions, with consistent binding preferences in locations relative to gene (Figure 2c). Despite similar binding site numbers and positional preferences, the overlap in binding sites between the DREB and ERF subfamilies was only about 50%, including core binding sites (Figure 2d). This highlights clear sequence differences in the DNA-binding sites between the two subfamilies.

All DREB/ERFs tend to bind to sequences containing a 7-bp core CCG motif; however, differences in the core motifs were observed between the DREB and ERF subfamilies (Figure 2e-g). Specifically, the core motif of the DREB subfamily was C(G/A)CCG(A/C)C, while that of the ERF subfamily was CGCCG(C/T)C (Figure 2e-g, Figure S4). Compared to ERF subfamily members, DREB subfamily members exhibited significant G/A variability at position 2 of the motif, with a predominant A base at position 6 (Figure 2e). In contrast, the core motif of ERF subfamily members features a conserved G base at position 2 and a variable C/T base at position 6, aligning with previous reports of DREB/ERF binding sequence motifs in other species (Yamasaki et al. 2013) (Figure 2e). Further motif analysis of binding sites specific to DREB, unique to ERF, and shared between the two subfamilies revealed that all are enriched in a core motif centred around CCG (Figure 2f-h).

It is worth noting that three group V members, which belong to the ERF subfamily—LITCHI030961, LITCHI016618, and LITCHI016922—exhibited A/G variability at position 2 of the core motif, similar to DREB members (Figure 2e), while the pattern at position 6 aligns with the ERF subfamily. Interestingly, their core motifs were consistent with those of the DREB subfamily rather than the ERF subfamily, suggesting that their binding and regulatory patterns were more similar to those of DREB subfamily members, despite their phylogenetic classification within the ERF subfamily (Figure 2g).

2.3 | Comparison of Potential Target Gene Sets Regulated by DREB/ERFs

Following our examination of the binding motif variations among the DREB/ERFs, we directed our attention toward investigating their potential target genes. Overall, a total of 23 973 potential genes were identified to be regulated by DREB/ERFs. Among them, 185 genes, referred to as core target genes, were jointly targeted by all 45 members of the DREB/ERF family (Figure 3a). The DREB and ERF subfamilies bind to 20953 and 20309 potential target genes, respectively, with core target gene counts of 279 for the DREB subfamily and 1326 for the ERF subfamily (Figure 3a). The number of target genes bound by different groups varies significantly, ranging from 3433 to 19005, with groups II, IX, and III targeting the largest numbers of genes (Figure 3b). Downstream target genes exhibited high variability among members of different subfamilies or groups. Correlation analysis of downstream binding sites across the 10 groups revealed significant differences



 $\label{eq:FIGURE1} \textbf{FIGURE 1} \quad | \quad \text{Legend on next page}.$

FIGURE 1 | Phylogenetic analysis of the DREB/ERF gene family in lychee. (a) Phylogenetic tree of the DREB/ERF gene family in lychee. 45 members marked with red dots have undergone DAP-seq analysis. The red and blue blocks represent the DREB and ERF subfamilies, respectively. The numbers next to the branches of the phylogenetic tree indicate bootstrap values. Gene IDs label the leaves of the phylogenetic tree, where DREB/ERF genes with 'm,' 'a,' or 'b' at the end have been manually corrected for structural annotation. Specifically, 'm' indicates errors or omissions in the original structural annotations, while 'a' and 'b' denote tandem duplicates that were incorrectly annotated as a single gene. (b) The key domains of the DREB/ERF proteins. The green rectangle represents the AP2 domain, while the horizontal axis indicates the length of the protein sequence. (c) Protein folding predictions (by Alphafold3) for the ten groups of DREB/ERFs. Each protein folding model represents one group of DREB/ERFs (I: LITCHI007962; II: LITCHI017494; III: LITCHI011765; IV: LITCHI010221; V: LITCHI016922; VI: LITCHI031037m; VII: LITCHI014444; VIII: LITCHI013895; IX: LITCHI008991a; X: LITCHI001614; blue: α-helix; red: β-sheet). (d) The reported biological functions of the orthologs of the ten lychee DREB/ERF groups in *Arabidopsis*. The biological processes represented by different icons are indicated at the bottom of the Figure 1.

(1-Jaccard Index > 0.5, Figure 3c, Figure S5a,c,e), which may be attributed to variations in the core motifs present in each group (Figures 2g and 3c). Although the overlap of binding sites among different groups was low, the overlap of potential downstream target genes was relatively high (1-Jaccard Index < 0.5), which was more pronounced between groups of the same subfamily (Figure 3d, Figure S5b,d,f). Notably, compared to other groups within the ERF subfamily, the target genes of group V aligned more closely with those of the DREB subfamily, suggesting that its biological regulatory functions may resemble those of DREB subfamily members.

GO enrichment analysis of the candidate target genes suggested that DREB/ERFs regulate various key biological processes, including responses to plant hormones such as ethylene, vegetative and reproductive growth and development, signal transduction, metabolism, and stress responses (Figure 3e). Additionally, there were differences in biological regulatory functions among different subfamilies, while groups within the same subfamily tend to show greater consistency (Figure 3e). Furthermore, lychee DREB/ERFs significantly bind to gene regions or candidate regulatory regions of multiple AP2 superfamily members such as AP2, which is involved in the differentiation of floral organs and the development of ovules and seed coats (Kunst et al. 1989; Ohto et al. 2009); AIL5, crucial for the developmental transition between embryonic and vegetative stages (Klucher et al. 1996); ERF4, which negatively regulates defence gene expression in response to jasmonic acid (JA) (McGrath et al. 2005); and CRF, which responds to cytokinin to regulate the development of embryos, cotyledons, and leaves (Rashotte et al. 2006)—exhibiting distinct binding patterns across subfamilies and groups (Figure 3f).

2.4 | DREB/ERFs Play a Broad Role in Reproductive Development in Lychee

Reproductive development, encompassing flower and fruit development, is a crucial biological process affecting lychee production. To further investigate the regulatory role of DREB/ERFs in lychee reproductive development, we integrated the DAP-seq dataset with publicly available RNA-seq data to identify DREB/ERFs that may play significant roles during reproductive development, along with their downstream regulatory networks and potential biological functions. Through transcriptomic analysis of five organs—leaves, flowers, seeds, pericarp, and aril—at different developmental stages in lychee, we identified numerous members with high-level or tissue-specific

expression patterns, hereinafter referred to as key DREB/ERFs (Figure S6, Figure 4a-e).

In leaves subjected to cold treatment (simulating vernalization), key DREB/ERFs generally showed decreased expression levels (Figure 4a). This subset of members may play a role in negatively regulating flowering in lychee. In the reproductive organs of male and female lychee flowers, most key DREB/ERFs tend to be highly expressed in the carpels and stamens of male and functional male flowers (Figure 4b). In contrast, *LITCHI008991b*, *LITCHI029903*, and *LITCHI029147* were highly expressed in the carpels of female flowers. During seed development, most key DREB/ERFs were highly expressed in the early stages (Figure 4c). In the development of the fruit skin and aril, most key DREB/ERFs show an increasing expression trend (Figure 4d,e), indicating that DREB/ERFs may primarily act to positively regulate lychee pericarp and aril development.

Among the key DREB/ERFs potentially involved in five major reproductive developmental processes-flowering, flower sex differentiation, seed development, pericarp development, and aril development—the number of those with completed DAP-seq sequencing is 16, 19, 16, 22, and 10, respectively (Figure 4a-e). A total of six DREB/ERFs exhibit high expression levels and significant variation in expression trends across the five reproductive developmental processes in lychee: LITCHI017494, LITCHI007962, LITCHI008991a, LITCHI029903, LITCHI014444, and LITCHI013895 (Figure 4a-f). This suggests that the six DREB/ERFs may serve as important regulatory factors in lychee reproductive development. Integration of DAP-seq and RNA-seq data identified numerous genes that are potentially regulated by DREB/ERFs in DAP-seq and exhibit a clear co-expression pattern with DREB/ERFs (Figure S7), indicating that these genes are likely directly regulated by DREB/ERFs at the transcriptional level. GO and KEGG enrichment analyses revealed that the downstream co-expressed target genes of these six DREB/ ERFs are enriched in several biological processes and pathways closely related to lychee flower and fruit development, including flower development, secondary metabolic pathways, embryo development, and carbohydrate metabolism (Figure 4g). Among these, a combination of phylogenetic analysis, expression profiling, and functional enrichment of the target gene set led us to the identification of an interesting gene, LITCHI017494. This gene belongs to group II, which is functionally associated with both terpene biosynthesis and flowering pathways. Therefore, we selected this gene as a representative example to investigate DREB/ERF transcription factor function in lychee growth and development.

2.5 | LITCHI017494 Regulates Sesquiterpenoid Biosynthesis in Lychee Aril

Aroma is an important quality trait of lychee fruit, with the aromatic compounds in the lychee aril primarily consisting of

terpenes (Liu et al. 2022; Hu et al. 2025). Our findings indicate that lychee DREB/ERFs regulate the biosynthesis of sesquiterpenoid in the lychee aril (Figure 5). Terpene synthase (TPS) is a key enzyme in the biosynthesis of terpenoid compounds (Chen et al. 2011). DAP-seq and RNA-seq integrative analysis

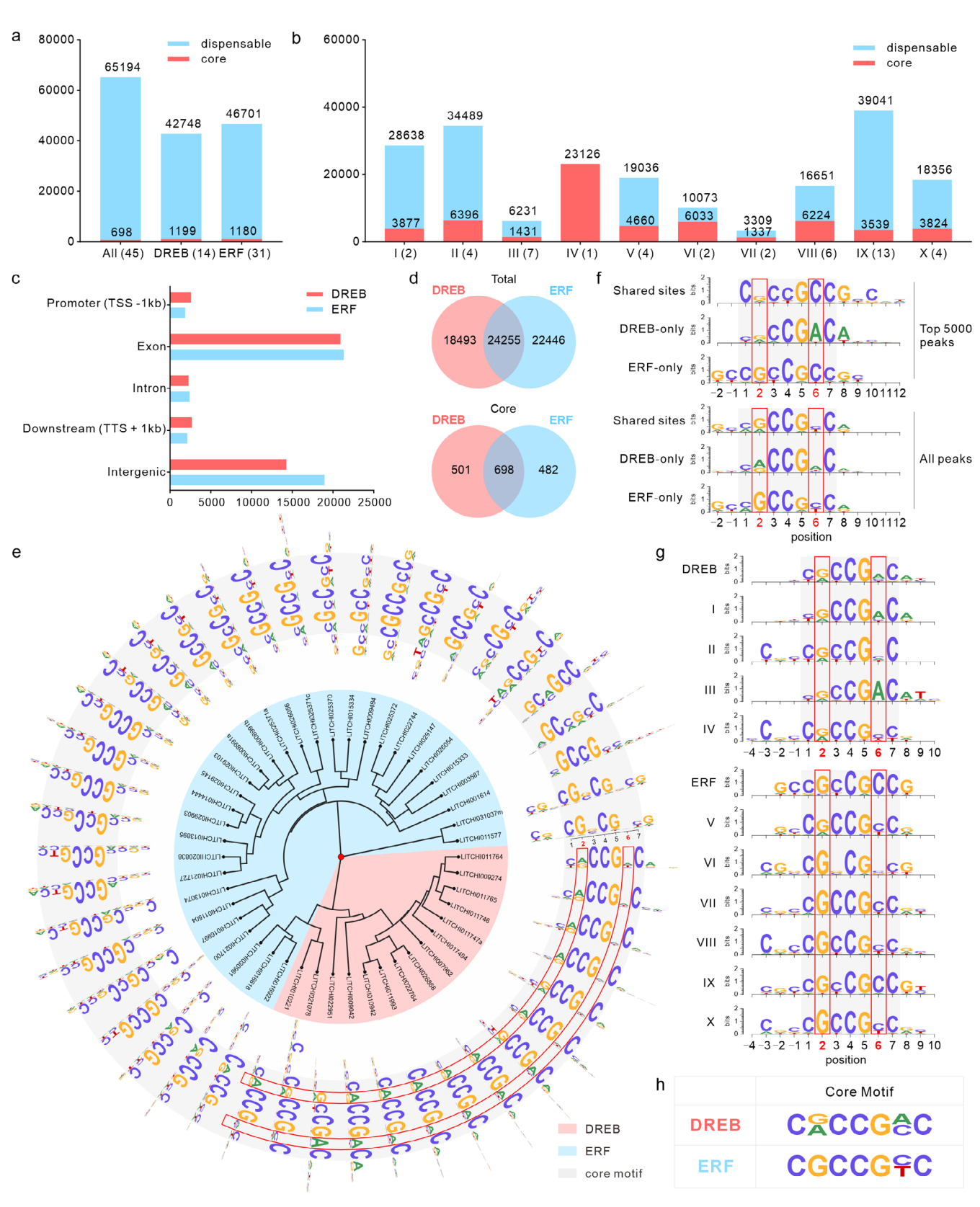


FIGURE 2 | Legend on next page.

FIGURE 2 | Overall characteristic of DREB/ERFs DNA-binding events in lychee. (a) The number of DNA-binding sites across the entire gene family and within each of the two subfamilies. Red squares indicate core sites bound by all members of the respective family or subfamily, while blue squares represent dispensable sites bound by only a subset of members. (b) The number of DNA-binding sites across the ten groups. (c) Distribution of peaks across different gene features in the DREB and ERF subfamilies. The vertical axis represents the positions of peaks relative to gene features, while the horizontal axis indicates the number of corresponding peaks. (d) Overlap of shared binding sites between the two subfamilies. (e) Top motif identified for each DREB/ERF member based on all peaks associated with each member, along with a dendrogram depicting motif sequence similarity among DREB/ERF members. (f) Top motif identified for shared sites, DREB-only subfamily sites, and ERF-only subfamily sites. (g) Top motif identified for binding sites across the two subfamilies and ten groups, based on the top 5000 peaks from each subfamily and group. (h) The 7-bp core motif of DREB and ERF binding sites in lychee.

revealed that LITCHI017494 is the DREB/ERF member in lychee that is highly expressed in lychee aril and simultaneously targets the first exon of three tandemly repeated *LcTPS*s (Figure 5a, Figure S8), suggesting that the LITCHI017494 protein may specifically bind to this exon region. The CDS sequences and protein functional domains of the three LcTPSs were largely consistent (Figure S9a,b), indicating that their protein functions were likely similar. The EMSA experiment confirmed that the GST-LITCHI017494 protein can bind to the predicted specific motif in the first exon of LcTPSs; the binding was lost when this motif was mutated, and the binding band weakened with the addition of competitive cold probes (Figure 5b, Figure S10). The yeast one-hybrid (Y1H) experiment further confirmed that LITCHI017494 can directly bind to the first exon of LcTPSs (Figure 5c). Similarly, dualluciferase reporter assay results supported LITCHI017494 activating the transcription of *LcTPS*s (Figure 5d). As predicted, LITCHI017494 was localised in the nucleus, functioning as a transcription factor (Figure 5e).

Additionally, the expression levels of *LITCHI017494* and *LcTPSs* followed the same trend, increasing significantly with the development and maturation of arils (Figure 5f). The expression levels of *LcTPSa2* and *LcTPSa1* were much higher than those of *LcTPSa3*, suggesting that they were the dominant TPS genes (Figure 5f). These results indicate that LITCHI017494 may promote terpenoid biosynthesis in lychee arils by up-regulating the expression of *LcTPSs*.

To confirm the function of LITCHI017494 and identify the biosynthetic compounds of LcTPSa2, we heterologously expressed *LITCHI017494* and *LcTPSa2* in tobacco leaves. Gas chromatography–mass spectrometry (GC–MS) analysis revealed that the biosynthetic product of LcTPSa2 was farnesol (Figure 5g), one of the main components previously reported in lychee aroma (Li et al. 2010). Additionally, LITCHI017494 promoted the biosynthesis of farnesol by LcTPSa2. In conclusion, LITCHI017494 promotes the biosynthesis of farnesol, a sesquiterpenoid in lychee aril, by up-regulating the transcription and expression of three tandemly repeated *LcTPSs*, thereby may influencing aroma formation in lychee aril.

2.6 | DREB/ERFs Act Differently in the Two Haplotypes of Lychee Genome With Different Maturation Period

Lychee (cultivar 'Feizixiao', 'FZX') exhibits two genomic haplotypes: early-maturing and late-maturing, suggesting differences in the flowering regulation pathways between them (Hu, Feng, et al. 2022). Given that DREB/ERFs may play an important role in the lychee flowering (Figure 4), we examined associations between lychee DREB/ERFs and maturation period by analysing DREB/ERF gene regulation across the two haplotypes representing different maturation periods. Between the HH haplotype (late-maturing) and the HY haplotype (early-maturing), the number of target genes bound by different DREB/ERF subfamilies and groups was generally consistent. However, compared to the reference genome without haplotype separation, there was a notable decrease in the number of identified target genes (Figure 3a,b, Figure S11). Consistency analysis showed significant differences in binding gene sets between the two haplotypes within the same group, with gene set differences ranging from 0.34 to 0.44 (Figure 6a).

GO enrichment analysis of binding genes revealed that genes within the same group exhibit varying enrichment in biological processes between the two haplotypes. These differences are closely related to several vital biological processes, including meristem transition, floral organ development, metabolic regulation, stress responses, signal transduction, and ethylene signalling responses. Notably, meristem transition is closely linked to flowering in lychee, which is directly associated with the maturation period (Figure 6b). These results indicate significant differences in gene binding and regulation of lychee DREB/ERFs between the two haplotypes, which are associated with the maturation period of lychee.

Further screening of flowering genes differentially regulated by lychee DREB/ERFs between the two haplotypes identified two important candidate genes, LcSVP and LcVOZ (Figure 6c,d), both of which exhibit differential binding by LITCHI017494 between the HH and HY haplotypes. LcSVP is a known negative regulator of flowering in lychee, and its function has been consistently confirmed in our studies (Figure S12) (Hu, Feng, et al. 2022; Huang et al. 2024). In the ninth exon, a SNP changes from A in the HH haplotype to T in the HY haplotype at the first position of the 7-bp core motif within the LITCHI017494 binding site. Consequently, LITCHI017494 specifically binds to LcSVP in the HH haplotype, but not to that in the HY haplotype (Figure 6c). LcVOZ is a direct homologue of AtVOZ1, which promotes flowering by downregulating FLC expression and upregulating FT expression (Celesnik et al. 2013; Yasui et al. 2012). In the first exon of LcVOZ, a SNP from A to C at position 3 of the 7-bp core motif in the LITCHI017494 binding site differentiates the HH and HY haplotypes. LITCHI017494 specifically binds to LcVOZ in the HY haplotype (Figure 6c). These differential

binding events were further confirmed through EMSA experiments (Figure 6e). In addition, luciferase assay experiments also indicated that LITCHI017494 significantly upregulates

the expression of *HH.LcSVP* and *HY.LcVOZ* (Figure 6f). These results suggest that base mutations in the 7-bp core motif enable LITCHI017494 to specifically bind to *HH.LcSVP* (whose

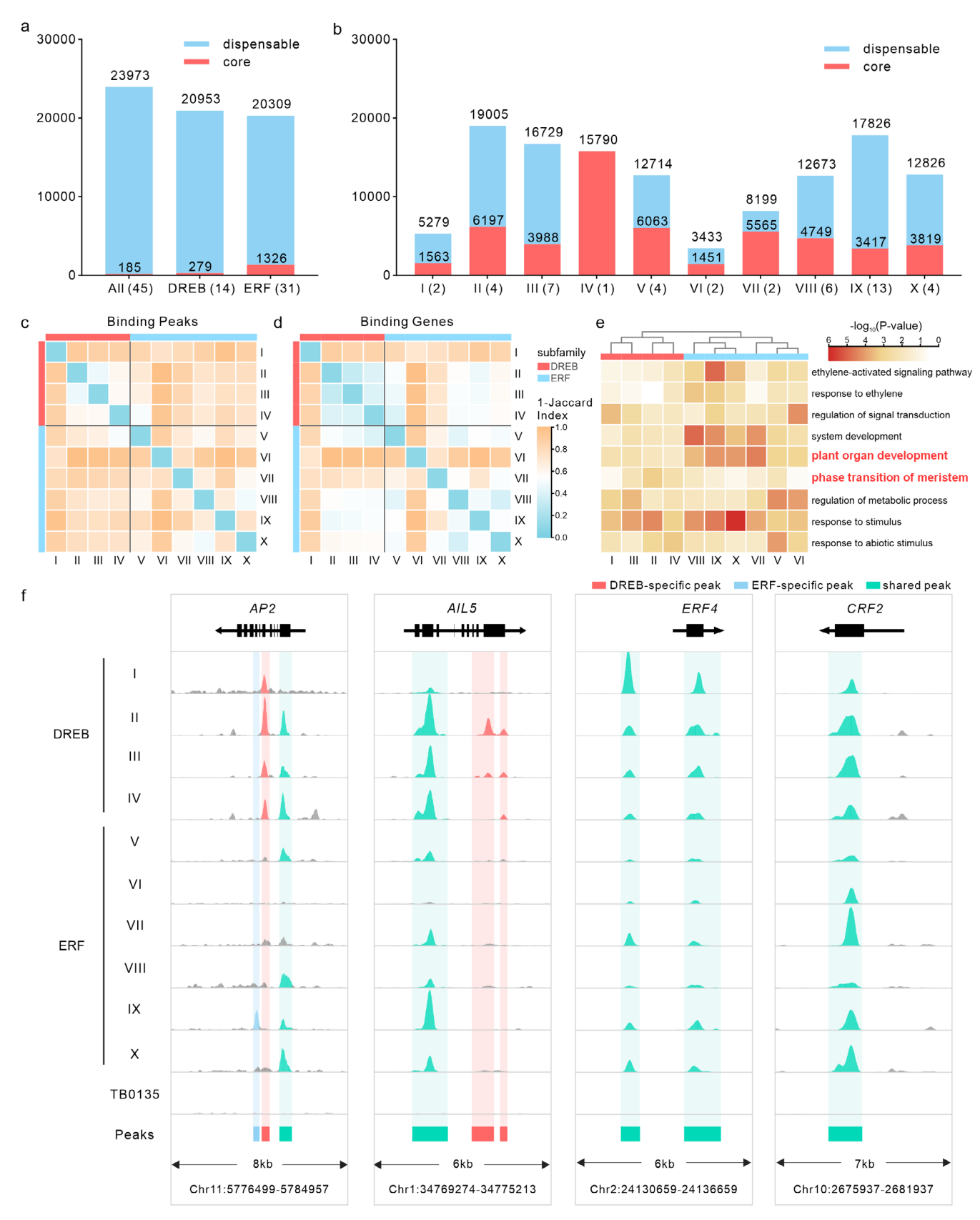


FIGURE 3 | Legend on next page.

FIGURE 3 | Lychee DREB/ERFs broadly bind to genes involved in key biological processes. (a) The number of binding genes across the entire gene family and within each of the two subfamilies. Red squares indicate core genes bound by all members of the respective family or subfamily, while blue squares represent dispensable genes bound by only a subset of members. (b) The number of binding genes across the ten groups. Target genes from all members within the same group were merged to remove redundancy, yielding the target gene set for that group. (c, d) Heatmap showing the correlation of DREB/ERF binding events among the ten groups (c: Binding peaks; d: Binding genes). '1-Jaccard Index' indicates the degree of difference between two groups, with values closer to 1 representing greater differences. (e) Predicted DREB/ERF target genes are enriched in GO functional terms related to ethylene, reproductive development, and other response processes. (f) DREB/ERF peaks are located in the putative regulatory regions of *AP2* genes and known ethylene-responsive genes. The y-axis ranges of DAP-seq read coverage were adjusted to 0–260, 0–600, 0–3200, and 0–1700 for *AP2*, *AIL5*, *ERF4*, and *CRF2*, respectively, to facilitate visualisation. The tracks labelled I to X show the reads and binding peaks from DAP-seq for the ten groups. For visualisation, one representative member from each group—selected based on the strongest DNA-binding ability—was chosen (I: LITCHI007962; II: LITCHI011746; III: LITCHI011765; IV: LITCHI010221; V: LITCHI016922; VI: LITCHI031037; VII: LITCHI011577; IX: LITCHI003587; X: LITCHI001614). The TB0135 track displays reads generated from the negative control sample. Coloured read coverage peaks in the DAP-seq signal tracks, along with the coloured squares at the bottom, correspond to called peaks: Red indicates DREB-specific peaks, blue indicates ERF-specific peaks, and green indicates peaks shared by both subfamilies.

expression is positively correlated with early flowering) and *HY.LcVOZ* (whose expression is negatively correlated with early flowering), thereby upregulating their expression.

Transcriptome analysis of winter leaves from 67 different lychee varieties with varying maturation periods reveals that the expression level of LITCHI017494 increases as the maturation period of the varieties is delayed. Correspondingly, the expression level of HH.LcSVP also shows an increasing trend, while the expression level of HY.LcVOZ exhibits a decreasing trend (Figure 6g). Additionally, population genotyping analysis indicates that lychee varieties with later maturity tend to have homozygous HH.LcSVP, while those with earlier maturity are more likely to exhibit homozygous HY.LcVOZ (Figure 6h). The high expression of the flowering inhibitory factor HH.LcSVP in late-maturing varieties and the high expression of the flowering promoter factor HY.LcVOZ in early-maturing varieties aligns with genotype and maturity characteristics of the varieties, with the effect of LcSVP being more pronounced at the transcriptional level (Figure 6h).

In conclusion, we speculate that LITCHI017494 is an important candidate gene in regulating the maturation period of lychee. A single base mutation in the core motif of the binding site for the downstream genes LcSVP and LcVOZ results in the specific up-regulation of LcSVP in the late-maturity haplotype, potentially delaying flowering and leading to later maturity. Conversely, the specific up-regulation of LcVOZ in early-maturing haplotypes may promote flowering and result in earlier maturation.

3 | Discussion

3.1 | Protein Structures and Critical Sites in Function Domains Align With DREB/ERF Sequence Evolution, and Define Binding Site Preference

Gene duplication followed by sub-functionalization and/or neofunctionalization is considered a key pathway for plant diversification and adaptation to diverse environmental conditions (Han et al. 2022). Investigating DNA-binding specificity across different family members offers valuable insights into genetic redundancy and diversity. The DNA-binding characteristics of each ERF protein are primarily determined by the structure of their DNA-binding domains (DBDs). This primary structural composition largely dictates how each ERF interacts with DNA, shaping its binding specificity and regulatory function. Phylogenetic classification within the ERF family goes beyond taxonomic grouping, potentially reflecting DNA-binding properties, as specific ERF subgroups tend to exhibit similar binding profiles and functional roles.

In lychee, DREB members feature a core structure comprising two α -helixes and a three-stranded β -sheet, while ERF members exhibit a core structure consisting of a single α -helix and a threestranded β-sheet, similar to their counterparts in Arabidopsis (Nakano et al. 2006) (Figure 1c, Figures S1b-d and S13b,c). Generally, genes within the same subfamily exhibit more conserved structures and functions. However, the protein structure and core binding motif of ERF group V align closely with those of the DREB subfamily, suggesting a binding regulation pattern similar to that of DREB subfamily members (Figure S1b-d, Figure 2g). This phenomenon is also observed in Arabidopsis (Figure S13). This result may be attributed to the evolutionary relationship between DREB and ERF, with DREB having originated from ERF through gene duplication and subsequent amplification (Han et al. 2022). Thus, Group V may represent a transitional form between ERF and DREB, as evidenced by the closer alignment of the 15th and 20th amino acids in the core AP2 domain with those of DREB (Figure S1a, Figure S12a).

In this study, we profiled downstream transcriptional targets for 45 representative lychee DREB/ERF members by DAP-seq, selecting at least one from each of the ten groups. Although representation across groups was not perfectly balanced, the set captures broad phylogenetic diversity and reflects expression during flower and fruit development. Within groups, target profiles were consistent: peak and gene binding correlation patterns for the strongest binder in each group closely matched those obtained by combining all available members (Figure S5). Members within the same group also shared more similar binding motifs (Figure S4), and within-group variation in binding events was lower than between-group variation (Figure S5e,f), indicating more conserved binding within groups. Therefore, these downstream binding profiles provide reliable coverage of the regulatory network of the DREB/ERF genes in lychee, especially in the context of their roles in flower and fruit development.

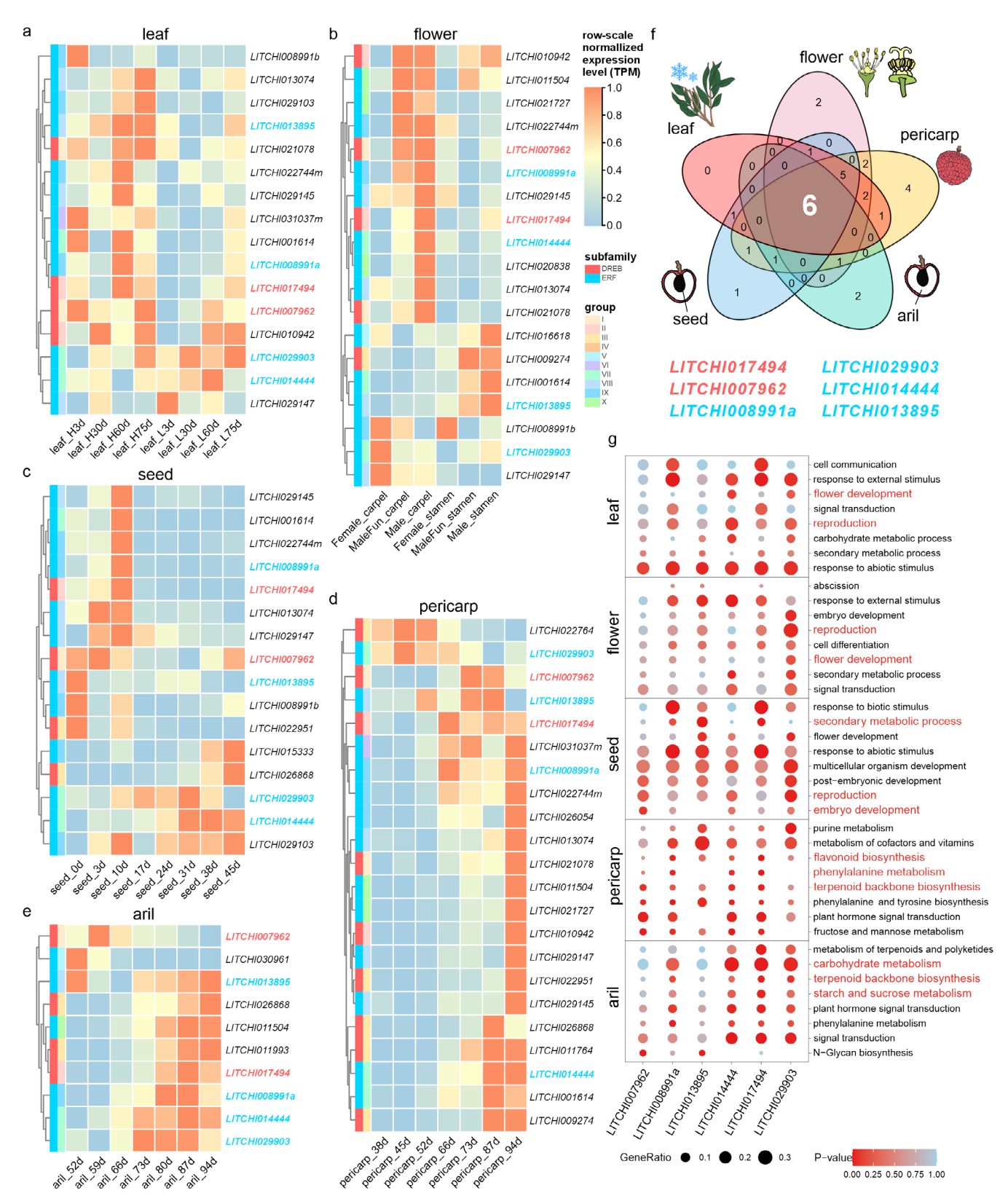


FIGURE 4 | DREB/ERFs are broadly involved in the development of flowers and fruits in lychee. (a–e) Key DREB/ERFs with high or specific expression patterns in five lychee organs: (a) leaves under different temperature treatments (leaf_H*: leaves of 'Nuomici' lychee trees under high temperature (25°C/20°C, day/night temperature, 12h day and 12h night); (eaf_L*: leaves under low temperature (15°C/8°C, day/night temperature, 12h day and 12h night)); (b) carpels and stamens of different sexual types of lychee flowers; (c) seeds of 'Huaizhi' at different developmental stages; (d) pericarp of 'Huaizhi' at different developmental stages; and (e) aril of 'Huaizhi' at different developmental stages. The expression levels (TPM) of key DREB/ERFs were normalised within rows. (f) Venn diagrams showing the overlap between key DREB/ERF sets across five organs, with six DREB/ERFs highly expressed in all five organs. (g) Genes predicted to be targets of the six key DREB/ERFs and co-expressed with them are enriched in GO terms related to reproductive development, secondary metabolism, signal transduction, and other response processes.

3.2 | ERFs Play a Pivotal Role in Terpenoid Biosynthesis Contributing to Attractive Aroma Across Diverse Plant Species

Recent studies have confirmed that ERF/DREB transcription factors are key regulators of plant growth and development,

particularly in controlling flowering and fruit maturation periods (Han et al. 2018; Hu, Sun, et al. 2022; Sun et al. 2024; Wei, Li, Lu, et al. 2022). This study also identified several ERF/DREB transcription factor members with high or specific expression patterns in lychee flowers and fruits, indicating that the DREB/ERF family plays a broad role throughout

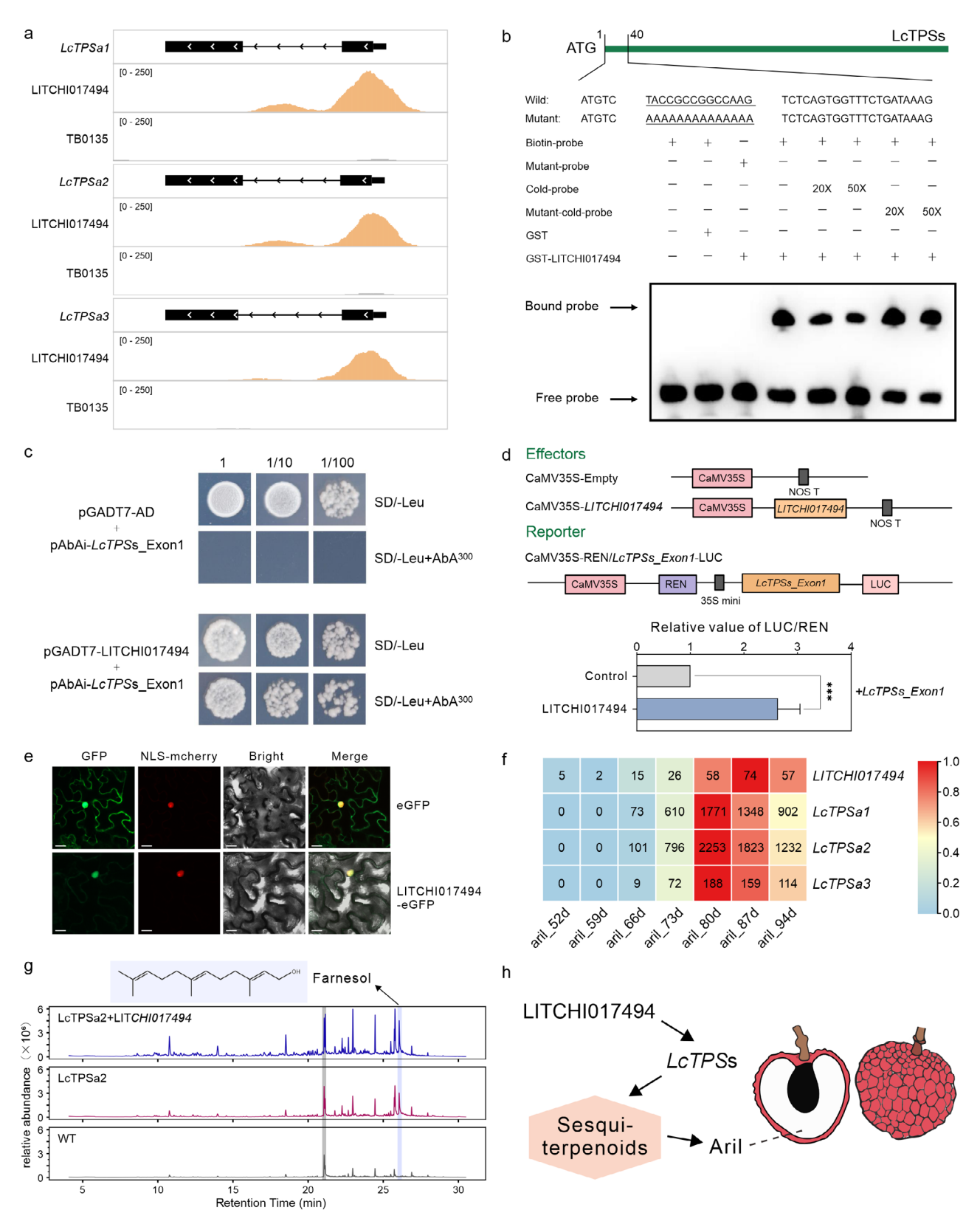


FIGURE 5 | Legend on next page.

FIGURE 5 | LITCHI017494 regulates sesquiterpenoid biosynthesis in lychee aril. (a) DAP-seq results show that LITCHI017494 binds to the first exon of three tandemly repeated *LcTPSs*. (b) Electrophoretic mobility shift assay (EMSA) shows that LITCHI017494 directly binds to motifs in the first exon of *LcTPSa1/2/3*. Recombinant purified LITCHI017494 protein (1μg) was incubated with biotin-labelled probes or with an unlabeled DNA probe containing intact (competitor) or mutated (mutant probe) binding motifs. (c) The Y1H assay reveals the binding of LITCHI017494 to specific fragments in the first exon of *LcTPSa1*. pGADT7-LITCHI017494 served as the prey, while pAbAi-*LcTPSa1_Exon1* was used as the bait. (d) LITCHI017494 activated the expression of *LcTPSa1-3* in vivo, as demonstrated by transient dual-luciferase reporter assays. Means and standard errors were calculated from three replicates (***p<0.001, two-sided Mann–Whitney test). (e) Subcellular localization of LITCHI017494 in *N. benthamiana* leaves. GFP: GFP channel; NLS-mCherry: Transgenic tobacco leaves with red fluorescence in the nucleus; Merge: merged image of the GFP and RFP channels; Bright-field: light microscopy image. Scale bars = 20μm. (f) Expression pattern of *LITCHI017494* and *LcTPSs* in lychee aril at different developmental stages. (g) Ectopic expression of *LITCHI017494* and *LcTPSa2* in *N. benthamiana* leaves. GC–MS analysis of farnesol from *N. benthamiana* leaves overexpressing *LITCHI017494* and *LcTPSa2*. *N. benthamiana* leaves transformed with pEAQ served as the control group (WT). Blue background: farnesol; Grey: ethyl caprate. (h) Proposed model of the LITCHI017494-*LcTPSs* regulatory pathway.

reproductive development, from flowering to fruit maturation (Figure 4a-e).

Terpenoids are the largest class of secondary metabolites in plants, with their biosynthesis typically catalysed by TPS enzymes through the MVA or MEP pathways (Sun et al. 2016). In lychee fruit, terpenoids are key contributors to the rose and citrus aroma (Liu et al. 2022). The synthesis of terpenoids is regulated by transcription factors, including members of the AP2/ ERF family. For example, the transcription factor PpERF61 controls linalool synthesis in peach by regulating the expression of PpTPS1 and PpTPS3 (Wei, Li, Cao, et al. 2022). In sweet orange, CitAP2.10 and CitERF71 modulate the biosynthesis of valencene and E-geraniol by upregulating CsTPS1 and CiTPS16, respectively (Li et al. 2017; Shen et al. 2016). In apples, MdMYC2 and MdERF3 activate the terminal enzyme MdAFS, regulating α -farnesene synthesis (Wang et al. 2020). In maize, ZmERE58 binds directly to the promoter of ZmTPS10, a gene involved in E- β -farnesene and E-α-bergamotene synthesis (Li et al. 2015). This study also found that LITCHI017494, a member of the DREB subfamily, which can directly bind to LcTPS genes (LcTPSa1, LcTPSa2, and LcTPSa3) in lychee to promote the synthesis of terpenoid acacia, thereby influencing the formation of fruit aroma (Figure 5). This implies that ERF transcription factors are broadly involved in regulating terpenoid synthesis across different plant species by modulating key biosynthetic enzymes.

3.3 | Differential Binding of ERF/DREB Transcription Factors to Haplotypes Regulates Flowering and Maturation Period in Lychee

In recent years, analysing the relationships between haplotype genomes and phenotypic polymorphism has emerged as a critical approach in crop breeding and variety improvement. For instance, in 2020, researchers revealed that while the two haplotypes of the alcohol acyltransferase gene *AAT1* in Gala apples share similar sequences, the expression level of haplotype A *AAT1* (derived from *Malus sylvestris*) is higher than that of haplotype B *AAT1* (derived from *Malus sieversii*), significantly influencing the aroma of ripe apples (Sun et al. 2020). Similarly, in 2023, a comparative analysis of the haplotype genomes of wild diploid bananas revealed that a 3 Mb translocation on chromosome 01 was associated with functions related to anther development, stamen development, and flower development (Liu et al. 2023).

Our previous studies on lychee have identified two genomic haplotypes associated with maturity timing: an early-maturing haplotype and a late-maturing haplotype, indicating potential variations in their floral regulation pathways (Hu, Feng, et al. 2022). Lychee varieties are categorised into three groups based on fruit maturity: extremely early-maturing cultivars (EEMC), early- and middle-maturing cultivars (EMC), and late-maturing cultivars (LMC) (Hu, Feng, et al. 2022). Notably, around 80% of lychee fruits ripen within a short window from early June to mid-July. Due to their short shelf life and high perishability, ensuring a consistent fresh supply throughout the year poses a significant challenge. Consequently, identifying key regulatory genes or genomic regions involved in the lychee fruit maturation period is crucial for improving its commercial value. In this study, we identified significant differences in the binding regulation between the two haplotypes of DREB/ERF transcription factors, which influenced the regulation of genes associated with the maturation period of lychee (Figure 6). Notably, this is the first study to identify a single-base mutation in the lychee haplotype genome that alters binding affinity, thereby shedding light on the molecular mechanisms underlying flowering in lychee.

The nucleic acid polymorphism at the binding site of ERFs is strongly associated with the fruit maturation period, making it a promising candidate for development as a molecular marker to support lychee-assisted breeding (Figure 6a). Extensive research on flowering regulation has identified short vegetative phase (SVP), a MADS-box transcription factor, as a potent flowering suppressor. SVP binds directly to the promoter region of flowering locus T (FT), inhibiting the expression of genes related to flowering (Lee et al. 2013, 2007). The suppression of LcSVP2 in developing lychee terminal buds had the effect of deferring dormancy re-entry, leading to a significantly reduced dormancy rate (Ma et al. 2024). Additionally, overexpression of lychee LcSVP2 or LcSVP10 in Arabidopsis results in a delayed flowering phenotype, signifying their potential role as flowering inhibitors (Ma et al. 2024; Pan et al. 2025). vascular plant one-zinc finger (VOZ) transcription factors, specifically VOZ1 and VOZ2, have been demonstrated to promote flowering in a redundant manner. Double mutants voz1 and voz2 exhibit late flowering phenotypes under long-day conditions, suggesting that VOZ1 and VOZ2 play overlapping roles in promoting flowering. VOZ1 and VOZ2 downregulate the expression of flowering locus C (FLC), a key repressor in the flowering pathway, thereby influencing flowering time

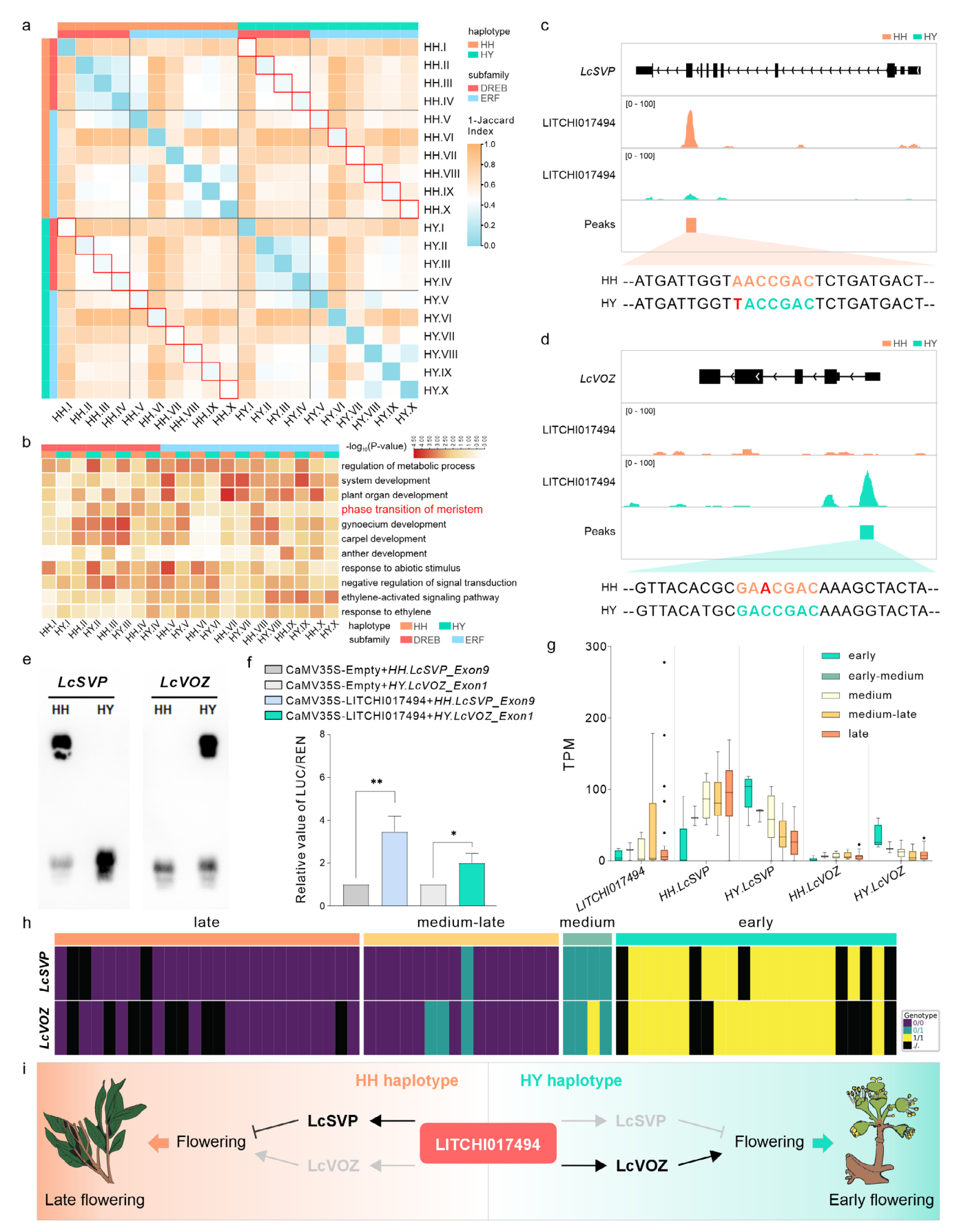


FIGURE 6 | Legend on next page.

FIGURE 6 | DREB/ERFs act differently in the two haplotypes of the lychee genome with different maturation periods. (a) Heatmap showing the correlation of lychee DREB/ERF gene-binding events among ten groups across the two haplotypes. (b) Predicted DREB/ERF target genes in the two haplotypes are enriched in GO terms related to ethylene, reproductive development, and metabolism. (c, d) LITCHI017494 exhibits differential binding to genes in the two haplotypes. (c: LcSVP; d: LcVOZ). (e) Electrophoretic mobility shift assay (EMSA) shows that LITCHI017494 directly binds to motifs in $HH.LcSVP_Exon9$ and $HY.LcVOZ_Exon1$. Recombinant purified GST-LITCHI017494 protein (1 μ g) was incubated with biotin-labelled probes or with an unlabeled DNA probe containing intact (competitor) or mutated (mutant probe) binding motifs. (f) LITCHI017494 activated the expression of HH.LcSVP and HY.LcVOZ in vivo, as demonstrated by transient dual-luciferase reporter assays. Means and standard errors were calculated from three replicates (**p<0.01, *p<0.05, two-sided Mann-Whitney test). (g) Transcript abundance of LITCHI017494, LcSVP, and LcVOZ in lychee cultivars with varying maturation periods. (h) LcSVP and LcVOZ exhibit different genotypes in lychee cultivars with varying maturation periods. Genotype 0/0 represents the HH/HH genotype, 0/1 represents the HH/HY genotype, 1/1 represents the HY/HY genotype, and ./. indicates an unknown genotype. (i) The regulatory model of LITCHI017494 in different haplotype genomes of lychee.

regulation (Celesnik et al. 2013; Yasui and Kohchi 2014; Yasui et al. 2012).

In this study, *LITCHI017494* was identified as a critical candidate gene involved in regulating the fruit maturation period of lychee by modulating the expression of *LcSVP* and *LcVOZ*. A single-base mutation within the core motif of its binding site for these downstream genes plays a pivotal role in determining ripening behaviour. In the late-ripening haplotype, this mutation specifically upregulates *LcSVP* expression, potentially delaying flowering and contributing to later ripening. Conversely, in early-maturing haplotypes, the same mutation upregulates *LcVOZ* expression, likely promoting flowering and resulting in earlier maturation (Figure 6c-h). These findings suggest that *LcERF* may directly bind to *LcSVP* and *LcVOZ*, thereby influencing the processes of flowering and the fruit maturation period in lychee.

3.4 | Haplotype-Specific Regulation by TFs in Highly Heterozygous Genomes Offers Promising Potential Applications

In this study, DREB/ERF transcription factors in lychee exhibited binding motif characteristics that are relatively conserved, similar to those observed in Arabidopsis and other plant species (Sakuma et al. 2002; Shoji et al. 2013). The core binding motif for the DREB subfamily is the DRE cis-element (5'-A/GCCGAC-3'), while that for the ERF subfamily is the typical GCC-box element (5'-AGCCGCC-3'). However, in contrast to herbaceous species such as Arabidopsis, which typically possess relatively homozygous genomes, a distinguishing feature of woody plants like lychee is their high level of genomic heterozygosity. The presence of haplotype-specific SNPs within binding motifs can readily alter the binding affinity of DREB/ERFs, thereby affecting their regulatory functions—as exemplified by the haplotype-specific transcriptional regulation of LITCHI017494 on LcSVP observed in this study (Figure 6). Allelic expression differences caused by cis-element variation are widespread and have a significant impact on the agronomic traits and environmental adaptability of plants. In lychee, sequence variation in the LcNAC1 binding site within the promoter of the terpene synthase gene *LcTPSa2* drives differences in farnesol biosynthesis by modulating the binding affinity of LcNAC1, thereby influencing the fruit's aroma (Hu et al. 2025). Similarly, four haplotype-specific SNPs within the A-box motif of the promoter of the maize COOL1 weaken the binding of bZIP transcription factors such as HY5,

reducing HY5-mediated repression of *COOL1* expression and thus enhancing the cold tolerance of maize (Zeng et al. 2025). Such haplotype-specific TF regulatory mechanisms, driven by extensive genomic heterozygosity, appear to be a common phenomenon in highly heterozygous plants and warrant increased attention from researchers in the field.

The integration of SNP genotyping into modern breeding has shifted selection from purely phenotypic to precision molecular design, supported by robust, cost-effective PCR-based platforms (e.g., CAPS, TaqMan, HRM, PACE, SNaPshot, KASP) (Kunihisa et al. 2003; Di Cristofaro et al. 2010; He et al. 2014; Słomka et al. 2017; von Maydell 2023). Marker-assisted selection (MAS), especially marker-assisted backcrossing (MABC), accelerates trait pyramiding and gene introgression with minimal linkage drag (Dormatey et al. 2020). For example, the salt-tolerance gene hst1 was precisely transferred into elite rice cultivars (Rana et al. 2019), and sequence-based SNP markers have aided introgression of disease resistance in wheat (Maccaferri et al. 2022; Song, Wang, et al. 2023). Additionally, SNP markers support population classification and germplasm management, as shown by 38 KASP SNPs used to define subpopulations in indica rice (Tang et al. 2022). This capability could extend to our applications, such as designing KASP markers based on the single-base mutation sites of the core motifs at the combination sites of *LcSVP* and *LcVOZ*. Such markers could classify lychee populations based on maturity period, thereby optimising parental selection strategies and enabling early, trait-based screening of hybrid progeny. This would facilitate optimised parental selection and early hybrid screening for target traits, thereby accelerating lychee breeding programs.

4 | Conclusion

In this study, we generated a global-scale profile of ERF binding site patterns through dozens of DAP-seq experiments. We uncovered binding motif preferences for each ERF phylogenetic group, providing robust evidence that aligns with ERF protein structures and critical peptide sites. An in-depth analysis of a specific lychee ERF gene revealed its role in the biosynthesis of aroma compounds and shed light on the complex transcriptional regulatory mechanisms in species with heterozygous genomes. The dataset generated in this study, along with the findings, will serve as a valuable resource and reference for transcription factor regulatory research within complex genomic contexts, especially for the ERF gene family.

5 | Materials and Methods

5.1 | Phylogenetic and Domain Analysis of DREB/ERF Gene Family in Lychee

To identify the DREB/ERF gene family in lychee, we used the peptide sequences of 114 DREB/ERF genes from the *Arabidopsis thaliana* genome database (http://www.arabidopsis.org/) as queries for a BLASTP (Altschul et al. 1990) search (*E*-value 1e-5) against the lychee longest peptide dataset, which was prepared using TBtools v2.136 (Chen et al. 2023). The genes obtained from the BLAST search were first corrected for gene structure annotation using IGV-GSAman (Chen, Li, et al. 2021), and then further aligned to the SwissProt database (UniProt Consortium 2019) to identify genes that could be aligned with the "Ethylene responsive transcription factor" (ERF) and were ultimately classified as the final lychee DREB/ERF gene set.

The longest peptide sequences of the final lychee DREB/ERF gene set were aligned and trimmed using MUSCLE v5.1 (Edgar 2004) and trimAl v1.4.rev15 (Capella-Gutiérrez et al. 2009) with default parameters. A phylogenetic tree was constructed using IQ-TREE v2.2.2.7 (Nguyen et al. 2015) with the following parameters: -m MFP -bb 1000 -bnni -st AA, and visualised using ChiPlot (Xie et al. 2023) (https://www.chiplot.online/).

The AP2 domain of each lychee DREB/ERF protein was identified using PfamScan v1.6 (El-Gebali et al. 2019) with default parameters. The AP2 domain was visualised using TBtools v2.136 (Chen et al. 2023), and the peptide sequences of the AP2 domain were aligned using MUSCLE v5.1 (Edgar 2004) and visualised with Jalview v2.11.4.1 (Waterhouse et al. 2009).

5.2 | Protein Modelling and Structure Analysis

The protein sequences of lychee DREB/ERFs were submitted to AlphaFold3 (Abramson et al. 2024) (https://deepmind.google/technologies/alphafold/alphafold-server/) for protein modelling, and then visualised and aligned using PyMOL (DeLano 2002).

5.3 | DAP-Seq Library Construction and Sequencing

The DNA affinity purification sequencing (DAP-seq) experiment was performed following the previously published protocols (Bartlett et al. 2017; O'Malley et al. 2016) with minor adjustments. Genomic DNA was extracted from young leaves of the lychee cultivar 'FZX', whose genome has been resolved into two haplotypes (Hu, Feng, et al. 2022), using the Cetyltrimethylammonium bromide (CTAB) method. The DNA samples were sonicated into fragments of approximately 200 bp using the Diagenode Bioruptor Pico, and the DNA fragments were then purified using AMPure XP beads (Beckman Coulter, A63880) according to the manufacturer's instructions. End repair and adapter ligation of the DNA fragments were performed using the NEBNext Ultra II End Repair/dA-Tailing and Ligation Module (NEB, E7546L, E7595L).

The coding sequences of *LcERFs* were amplified by PCR using cDNA from 'FZX' as the template, with the corresponding PCR primers listed in Table S2. The PCR products were then cloned into the pIX-Halo vector to produce LcERF-Halo fusion proteins in vitro using the TNT SP6 High-Yield Wheat Germ Protein Expression System (Promega, L3260). HaloTag magnetic beads (Promega, G7282) were used to pull down the LcERF-Halo fusion proteins.

The purified LcERF-Halo fusion proteins were incubated with the adaptor-ligated DNA library from 'FZX' at 1500 rpm, 25°C for 1h. After incubation, the complexes were washed three times with PBS buffer, and the DNA fragments were eluted with EB solution. Sequencing was performed on a NovaSeq 6000 with 150 bp paired-end reads. Each sample was replicated twice.

5.4 | Read Mapping

Fastq files were trimmed using Trimmomatic v0.39 (Bolger et al. 2014) with the following parameters: ILLUMINACLIP: Merged.adapter.fa:2:30:10, TRAILING:3, SLIDINGWINDOW:4:15, MINLEN:25, MAXINFO:76:0.6. Trimmed reads were mapped to the lychee reference genome and haplotype-resolved assemblies (Hu, Feng, et al. 2022), respectively, using Bowtie2 v2.5.3 (Langmead and Salzberg 2012).

5.5 | Peak Calling, Merging and Visualisation

Peaks were called using MACS2 v2.2.9.1 (Zhang et al. 2008) with the pIX-Halo (TB0135) negative control sample for background subtraction and a minimum FDR (q-value) cutoff of 0.00001 (-q 0.00001). Peak calling was performed with the following parameters: -g 469 438 100 -B -f BAMPE -n R -q 0.00001.

Datasets generated from DREB/ERFs that belong to the same subfamily or group were merged using the custom script find-commonpeaks.py. With a bin size of 50 bp, the continuous bins occupied by peaks from any dataset of a specific subfamily or group were defined as the binding peak regions of the subfamily or group. Core and dispensable peaks for each subfamily and group were assigned using the custom script peakcluster.py.

For visualisation, BAM files were converted to bedGraph files using deepTools v3.5.3 (Ramírez et al. 2014) bamCoverage with a 10 bp bin size. Genes and binding reads of specified genomic regions were visualised (Figure 3f) using custom scripts coveragevisualization.py.

Correlation of DREB/ERF binding peaks among the ten groups was calculated using custom script correlation.py. Venn diagrams and heatmaps were drawn using TBtools v2.136 (Chen et al. 2023).

5.6 | Motif Enrichment Analysis

The most highly enriched motif for each individual DREB/ERF dataset, group dataset, and subfamily dataset (generated for lychee reference genome) was determined using MEME-ChIP

v5.5.5 (Machanick and Bailey 2011) with the following parameters: -meme-mod anr -meme-minsites 10 -meme-maxsites 12 -minw 10 -maxw 12 -meme-nmotifs 3. Fasta sequence files required as input for meme-chip were generated by extracting 50bp upstream and downstream of the peak summit (from peaks with pileup \geq 5, $-\log_{10}(p \text{ value}) \geq$ 5, fold enrichment \geq 2) using the TBtools v2.136 (Chen et al. 2023). Motif logos were generated using MotifStack (Ou et al. 2018).

5.7 | Target Gene Identification and GO Analysis

Peak position relative to gene features was assigned using the custom script peakAnno.py. Promoter-regulatory region (Figure 2c) was defined as 1kb upstream of the transcription start site (TSS) and downstream-regulatory region as 1kb downstream of the transcription termination site (TTS) and gene bodies (exons including 5'-and 3'-UTRs, and introns). Longest transcripts were generated from the lychee reference genome and lychee haplotype-resolved genome assemblies using TBtools v2.136 (Chen et al. 2023) and were used for most analyses. Target genes were defined as the closest genes containing a peak within 1kb +100bp upstream of the TSS and 1kb -100bp downstream of the TTS (or in the UTR). GO enrichment was performed using TBtools v2.136 (Chen et al. 2023) and visualised using ggplot2 (https://ggplot2.tidyverse.org).

5.8 | Transcriptome Data Analysis

Transcriptome data of lychee leaf, flower, aril, and seed were downloaded from the SRA database (Guan et al. 2021; Lu et al. 2022; Zhang, Zeng, et al. 2024). Transcriptome data of lychee pericarp was generated in this study. Total RNA was extracted using PureLink Plant RNA purification Reagent (Invertrogen, Code No: 12322012) from 'Huaizhi' lychee pericarp; 1 µg high-quality RNA from 7 samples with high quality was sent to BioMaker (China, Beijing) for mRNA library construction and RNA sequencing (RNA-seq). In total, 7 pericarp mRNA libraries were constructed and sequenced on a NovaSeq 6000 platform.

Quality control of raw data was conducted using FastQC v0.12.1 (https://www.bioinformatics.babraham.ac.uk/projects/fastqc/) to confirm acceptable quality for downstream analysis. Trimmomatic v0.39 (Bolger et al. 2014) was invoked to remove the low-quality bases present in the sequencing data at the 3' end of the splice sequence and read segment. All sequence data were compared to the lychee reference genome and haplotyperesolved assemblies respectively using STAR v2.7.11b (Dobin et al. 2013, respectively). The expression of genes was calculated using StringTie v2.2.3 (Pertea et al. 2015) and normalised to TPM. Weighted Gene Co-Expression Network Analysis (WGCNA) was conducted using R package WGCNA v1.71 (Langfelder and Horvath 2008).

5.9 | Electrophoretic Mobility Shift Assay (EMSA)

The coding sequence of *LITCHI017494* was cloned into the pGEX-4T-1 vector using the primers listed in Table S3 and then was expressed in *Escherichia coli* Rosseta (DE3). Expression and purification of the recombinant protein were performed according

to the GST-tag Protein Purification Kit (Beyotime) manufacturer's instructions. The EMSA was conducted using the LightShift Chemiluminescent EMSA Kit (Thermo Fisher Scientific) (Zhang, Zeng, et al. 2024). The double-stranded probes with 3' biotin labelling were made by annealing separately synthesised strands. The probes used for EMSAs are listed in Table S3.

5.10 | Yeast One-Hybrid Assay

The first exon of *LcTPSs* was cloned into the pAbAi vector, and the construct was integrated into the genome of the Y1HGold yeast strain. The background aureobasidin A resistance (AbA^I) expression of Y1HGold LcTPSs-Exon1-pAbAi strain was tested on selective synthetic dextrose medium (SD) uracil. Then, the full length of *LITCHI017494* was cloned into the pGADT7 vector for identification. After determining the minimal inhibitory concentration of AbA for the bait strains, the AD prey vectors were transformed into the bait strain and screened on an SD/Leu/AbA plate. Individual bait-prey interactions were performed to verify the positive recombined prey vector. All transformations and screenings were examined at least three times. Primers used in this assay are listed in Table S3.

5.11 | Dual-Luciferase Reporter Assays

According to the previous protocol (Wei, Li, Lu, et al. 2022; Zhang, Zeng, et al. 2024), full-length CDS of transcription factor, *LITCHI017494*, was cloned into pGreen II 62-SK vector as the effector, and the first exon of *LcTPSs* was cloned into pGreen II 0800-LUC vector as the reporters using the primers listed in Table S3. The above effector and reporter constructs were transformed into *A. tumefaciens* GV3101::pSoup, and the bacteria were injected into tobacco leaves for transient expression assays. After 3 days infiltration, the leaf zones of infiltration were harvested for enzyme activity assays of firefly luciferase and renilla luciferase using the DualLuciferase Reporter Assay System (YEASEN, Shanghai, China). At least three independent biological replicates were performed.

5.12 | Subcellular Localization Analysis

The recombined 35S-LITCHI017494-GFP vectors were constructed using primers listed in Table S3 and were transformed into Agrobacterium tumefaciens GV3101::pSoup for transient expression in tobacco (Nicotiana benthamiana) leaves. The vector was infiltrated into transgenic tobacco leaves expressing a red fluorescent nuclear marker (Nucleus-RFP). After 48 h infiltration, the leaves were detached for analysis using a confocal laser scanning microscope (LSM 800; Carl Zeiss, Oberkochen, Germany). The acquired images were processed with the LSM Image Browser (Carl Zeiss). The experiment was conducted in triplicate.

5.13 | Transient Expression of *LcTPSa2* and *LITCHI017494* in *N. Benthamiana*

The full-length CDSs of *LcTPSa2* and *LITCHI017494* genes were cloned into the pEAQ-HT-DEST-1 expression vector using the

primers in Table S3, respectively. The pEAQ-HT-DEST-1 vector used for transient expression study in N. benthamiana was kindly donated by Dr. Zhenhua Liu at Shanghai Jiao Tong University. Expression vectors were introduced into A. tumefaciens strain LBA4404. The bacteria were re-suspended in infiltration buffer (10 mM MES, 10 mM MgCl₂, 150 μM acetosyringone, pH 5.6) at $OD_{600} = 0.65$ and incubated for 3h at room temperature. After 5 days, infected leaves of N. benthamiana were extracted according to a previous report (Wu et al. 2019). Tobacco leaves (1g) were ground and homogenised in a 30 mL saturated salt solution. After centrifuging for 20 min at 13000 g, the supernatant was used as the crude extract. Isolation of glycosidic precursors was conducted by using SPE LC-18 resins (CNW, Duesseldorf, Germany). Elimination of free volatile compounds was accomplished by washing with 25 mL of dichloromethane, and the bound fraction was eluted with 25 mL of methanol. The bound volatile compounds were enzymatically hydrolyzed at 40°C after adding 2 mg of β-D-Glucoside glucohydrolase (CAS: 9001-22-3, Sigma-Aldrich) according to previous studies (Bönisch et al. 2014; Yauk et al. 2014). The free aglycones were released for 30 min at 45°C and collected using a solid-phase microextraction (SPME) fibre coated with 100 µm of polydimethylsiloxane and divinylbenzene (PDMS-DVB, 3 pk (Red)) (Supelco Inc., Bellefonte, PA, USA). The released volatiles were identified using GC-MS.

An Agilent 7890B gas chromatograph coupled with an Agilent 5977A mass spectrophotometer (Agilent, Palo Alto, CA, USA) equipped with a HP-5MS column (0.30 mm, 30 m, 0.25 μ m, J&W Scientific, Folsom, CA, USA) was applied for identification of volatile compounds according to methods described. Helium was used as a carrier gas at a flow rate of $1.0\,\mathrm{mL\,min^{-1}}$. The temperature program started at $40^\circ\mathrm{C}$ and was increased by $8^\circ\mathrm{C}$ min $^{-1}$ to $100^\circ\mathrm{C}$ and then to $240^\circ\mathrm{C}$ at $10^\circ\mathrm{C}$ min $^{-1}$. The column effluent was ionised by electron ionisation (EI) at an energy of $70\,\mathrm{eV}$, and the source temperature was $230^\circ\mathrm{C}$. Mass scanning was done over the range 35-550 aum. Volatile compounds were identified by comparing their EI mass spectra with the NIST Mass Spectral Library (NIST14.L) and the retention time of authentic standards.

5.14 | Transgenic Arabidopsis Generation

As described in Huang et al. (2024), we generated transgenic *Arabidopsis* (Col-0) plants by cloning the *LcSVP* coding sequence into the pEarleyGate 201 binary vector downstream of the CaMV 35S promoter. The recombinant construct was transformed into *Agrobacterium tumefaciens* strain GV3101, which was then used to transform homozygous *svp-31* mutant plants (SALK_026551; obtained from the Arabidopsis Biological Resource Center (ABRC) (Alonso et al. 2003)) via the floral dip method. Primary transformants (T1 generation) were selected using BASTA, with successful transformants confirmed by PCR genotyping.

5.15 | Population SNP Calling

This study utilised the re-sequencing data of 68 lychee accessions from a previous investigation (Hu, Feng, et al. 2022) (Table S4).

The reads were aligned to the lychee reference genome using BWA-MEM v0.7.17 (Li 2013), and the alignments were sorted by genomic position with SAMtools v1.16.1 (Li et al. 2009). Duplicate reads were removed using Picard v2.12.1 (http://broadinstitute.github.io/picard/). Variant calling and joint genotyping were performed with GATK v4.1.2.0 (McKenna et al. 2010). Specifically, GATK HaplotypeCaller was used to generate gVCF files for each sample, and GATK GenotypeGVCFs was applied to combine variants across all samples. High-quality variants were obtained by applying GATK SelectVariants to filter out variants based on the following criteria: QD <2.0, QUAL <30.0, SOR >3.0, FS>60.0, MQ <40.0, MQRankSum <-12.5, or ReadPosRankSum <-8.0.

Author Contributions

F.W., C.C., R.X., and Z.Z. conceived and designed the project; F.W., H.L., J.F., and C.C. performed the bioinformatics data analysis. J.Z., H.H., Y.X., and Z.Z. conducted the experiments. F.W., J.Z., H.H., Y.H., C.C., R.X., and Z.Z. prepared the figures and wrote the manuscript. All authors read and approved the final manuscript.

Acknowledgements

This work is supported by the Key Area Research and Development Program of Guangdong Province (2022B0202070003), the National Science Foundation of China (#32072547, #32372665, and #32102320), and the Project of State Key Laboratory of Tropical Crop Breeding (SKLTCBZRJJ202502). We gratefully acknowledge the support of the Bioinformatics Facility in the Collage of Horticulture at SCAU. We also thank Yin Huanhuan for technical assistance with gene cloning.

Conflicts of Interest

The authors declare no conflicts of interest.

Data Availability Statement

The DAP-seq sequencing data can be found in the Sequence Read Archive under accession number PRJNA1204501. The RNA sequencing data can be found in the Sequence Read Archive under accession numbers PRJNA1204918, PRJNA766549, PRJNA766599, PRJNA756275, and PRJNA1163705. The re-sequencing data can be found in the Sequence Read Archive under accession number PRJNA747875. The datasets generated and analysed during the current study are available at figshare (10.6084/m9.figshare.28114127). The custom scripts used in this paper can be found at GitHub (https://github.com/yanyew/Custom-DAP-seq-analysis-scripts).

References

Abramson, J., J. Adler, J. Dunger, et al. 2024. "Accurate Structure Prediction of Biomolecular Interactions With AlphaFold 3." *Nature* 630: 493–500.

Alonso, J. M., A. N. Stepanova, T. J. Leisse, et al. 2003. "Genome-Wide Insertional Mutagenesis of *Arabidopsis thaliana*." *Science* 301: 653–657.

Altschul, S. F., W. Gish, W. Miller, E. W. Myers, and D. J. Lipman. 1990. "Basic Local Alignment Search Tool." *Journal of Molecular Biology* 215: 403–410.

Bartlett, A., R. C. O'Malley, S.-s. C. Huang, et al. 2017. "Mapping Genome-Wide Transcription-Factor Binding Sites Using DAP-Seq." *Nature Protocols* 12: 1659–1672.

Bolger, A. M., M. Lohse, and B. Usadel. 2014. "Trimmomatic: A Flexible Trimmer for Illumina Sequence Data." *Bioinformatics* 30: 2114–2120.

- Bönisch, F., J. Frotscher, S. Stanitzek, et al. 2014. "Activity-Based Profiling of a Physiologic Aglycone Library Reveals Sugar Acceptor Promiscuity of Family 1 UDP-Glucosyltransferases From Grape." *Plant Physiology* 166: 23–39.
- Capella-Gutiérrez, S., J. M. Silla-Martínez, and T. Gabaldón. 2009. "trimAl: A Tool for Automated Alignment Trimming in Large-Scale Phylogenetic Analyses." *Bioinformatics* 25: 1972–1973.
- Celesnik, H., G. S. Ali, F. M. Robison, and A. S. Reddy. 2013. "*Arabidopsis thaliana* VOZ (Vascular Plant One-Zinc Finger) Transcription Factors Are Required for Proper Regulation of Flowering Time." *Biology Open* 2: 424–431.
- Chen, C., J. Li, J. Feng, et al. 2021. "sRNAanno—A Database Repository of Uniformly Annotated Small RNAs in Plants." *Horticulture Research* 8: 45.
- Chen, C., Y. Wu, J. Li, et al. 2023. "TBtools-II: A "One for All, All for One" Bioinformatics Platform for Biological Big-Data Mining." *Molecular Plant* 16: 1733–1742.
- Chen, F., D. Tholl, J. Bohlmann, and E. Pichersky. 2011. "The Family of Terpene Synthases in Plants: A Mid-Size Family of Genes for Specialized Metabolism That Is Highly Diversified Throughout the Kingdom." *Plant Journal* 66: 212–229.
- Chen, Y., L. Zhang, H. Zhang, L. Chen, and D. Yu. 2021. "ERF1 Delays Flowering Through Direct Inhibition of Flowering Locus T Expression in *Arabidopsis*." *Journal of Integrative Plant Biology* 63: 1712–1723.
- DeLano, W. L. 2002. "Pymol: An Open-Source Molecular Graphics Tool." *CCP4 Newsletter on Protein Crystallography* 40: 82–92.
- Deng, D., Y. Guo, L. Guo, et al. 2024. "Functional Divergence in Orthologous Transcription Factors: Insights From AtCBF2/3/1 and OsDREB1C." *Molecular Biology and Evolution* 41: msae089.
- Di Cristofaro, J., M. Silvy, J. Chiaroni, and P. Bailly. 2010. "Single PCR Multiplex SNaPshot Reaction for Detection of Eleven Blood Group Nucleotide Polymorphisms: Optimization, Validation, and One Year of Routine Clinical Use." *Journal of Molecular Diagnostics* 12: 453–460.
- Dobin, A., C. A. Davis, F. Schlesinger, et al. 2013. "STAR: Ultrafast Universal RNA-Seq Aligner." *Bioinformatics* 29: 15–21.
- Dormatey, R., C. Sun, K. Ali, J. A. Coulter, Z. Bi, and J. Bai. 2020. "Gene Pyramiding for Sustainable Crop Improvement Against Biotic and Abiotic Stresses." *Agronomy* 10: 1255.
- Durán-Medina, Y., J. Serwatowska, J. I. Reyes-Olalde, S. De Folter, and N. Marsch-Martínez. 2017. "The AP2/ERF Transcription Factor DRNL Modulates Gynoecium Development and Affects Its Response to Cytokinin." *Frontiers in Plant Science* 8: 1841.
- Edgar, R. C. 2004. "MUSCLE: Multiple Sequence Alignment With High Accuracy and High Throughput." *Nucleic Acids Research* 32: 1792–1797.
- El-Gebali, S., J. Mistry, A. Bateman, et al. 2019. "The Pfam Protein Families Database in 2019." *Nucleic Acids Research* 47: D427–D432.
- Feng, K., X.-L. Hou, G.-M. Xing, et al. 2020. "Advances in AP2/ERF Super-Family Transcription Factors in Plant." *Critical Reviews in Biotechnology* 40: 750–776.
- Guan, H., H. Wang, J. Huang, et al. 2021. "Genome-Wide Identification and Expression Analysis of MADS-Box Family Genes in Litchi (*Litchi chinensis* Sonn.) and Their Involvement in Floral Sex Determination." *Plants* 10: 2142.
- Han, J., X. Xie, Y. Zhang, et al. 2022. "Evolution of the Dehydration-Responsive Element-Binding Protein Subfamily in Green Plants." *Plant Physiology* 190: 421–440.
- Han, Z., Y. Hu, Y. Lv, et al. 2018. "Natural Variation Underlies Differences in Ethylene Response Factor17 Activity in Fruit Peel Degreening." *Plant Physiology* 176: 2292–2304.

- He, C., J. Holme, and J. Anthony. 2014. "SNP Genotyping: The KASP Assay." In *Crop Breeding: Methods and Protocols*, 75–86. Springer New York.
- He, Z., X. Ma, F. Wang, J. Li, and M. Zhao. 2023. "LcERF10 Functions as a Positive Regulator of Litchi Fruitlet Abscission." *International Journal of Biological Macromolecules* 250: 126264.
- Hu, G., J. Feng, X. Xiang, et al. 2022. "Two Divergent Haplotypes From a Highly Heterozygous Lychee Genome Suggest Independent Domestication Events for Early and Late-Maturing Cultivars." *Nature Genetics* 54: 73–83.
- Hu, H., H. Liu, Z. Zeng, et al. 2025. "Genetic Variation in a Tandemly Duplicated TPS Gene Cluster Contributes to the Diversity of Aroma in Lychee Fruit." *New Phytologist* 246: 2652–2665.
- Hu, Y., H. Sun, Z. Han, et al. 2022. "ERF4 Affects Fruit Ripening by Acting as a JAZ Interactor Between Ethylene and Jasmonic Acid Hormone Signaling Pathways." *Horticultural Plant Journal* 8: 689–699.
- Huang, X., H. Liu, F. Wu, et al. 2024. "Diversification of FT-Like Genes in the PEBP Family Contributes to the Variation of Flowering Traits in Sapindaceae Species." *Molecular Horticulture* 4: 28.
- Huang, Y., X. Xing, Y. Tang, et al. 2022. "An Ethylene-Responsive Transcription Factor and a Flowering Locus KH Domain Homologue Jointly Modulate Photoperiodic Flowering in Chrysanthemum." *Plant, Cell & Environment* 45: 1442–1456.
- Kagaya, Y., K. Ohmiya, and T. Hattori. 1999. "RAV1, a Novel DNA-Binding Protein, Binds to Bipartite Recognition Sequence Through Two Distinct DNA-Binding Domains Uniquely Found in Higher Plants." *Nucleic Acids Research* 27: 470–478.
- Klucher, K. M., H. Chow, L. Reiser, and R. L. Fischer. 1996. "The Aintegumenta Gene of *Arabidopsis* Required for Ovule and Female Gametophyte Development Is Related to the Floral Homeotic Gene *APETALA2*." *Plant Cell* 8: 137–153.
- Kunihisa, M., N. Fukino, and S. Matsumoto. 2003. "Development of Cleavage Amplified Polymorphic Sequence (CAPS) Markers for Identification of Strawberry Cultivars." *Euphytica* 134: 209–215.
- Kunst, L., J. E. Klenz, J. Martinez-Zapater, and G. W. Haughn. 1989. "AP2 Gene Determines the Identity of Perianth Organs in Flowers of *Arabidopsis thaliana*." *Plant Cell* 1, no. 12: 1195–1208.
- Langfelder, P., and S. Horvath. 2008. "WGCNA: An R Package for Weighted Correlation Network Analysis." *BMC Bioinformatics* 9: 1–13.
- Langmead, B., and S. L. Salzberg. 2012. "Fast Gapped-Read Alignment With Bowtie 2." *Nature Methods* 9: 357–359.
- Lee, J. H., H.-S. Ryu, K. S. Chung, et al. 2013. "Regulation of Temperature-Responsive Flowering by MADS-Box Transcription Factor Repressors." *Science* 342: 628–632.
- Lee, J. H., S. J. Yoo, S. H. Park, I. Hwang, J. S. Lee, and J. H. Ahn. 2007. "Role of SVP in the Control of Flowering Time by Ambient Temperature in *Arabidopsis*." *Genes & Development* 21: 397–402.
- Li, C., J. Hao, H. Zhong, and Y. Xu. 2010. "Free and Glycosidically Bound Volatile Flavor Compounds in Fruit of *Litchi chinensis* 'Huaizhi'." *Food Science* 31: 268–271.
- Li, H. 2013. "Aligning Sequence Reads, Clone Sequences and Assembly Contigs With BWA-MEM." arXiv preprint arXiv:1303.3997.
- Li, H., B. Handsaker, A. Wysoker, et al. 2009. "The Sequence Alignment/Map Format and SAMtools." *Bioinformatics* 25: 2078–2079.
- Li, S., H. Wang, F. Li, et al. 2015. "The Maize Transcription Factor EREB 58 Mediates the Jasmonate-Induced Production of Sesquiterpene Volatiles." *Plant Journal* 84: 296–308.
- Li, X., Y. Xu, S. Shen, et al. 2017. "Transcription Factor CitERF71 Activates the Terpene Synthase Gene CitTPS16 Involved in the Synthesis

- of E-Geraniol in Sweet Orange Fruit." *Journal of Experimental Botany* 68: 4929–4938.
- Liu, X., R. Arshad, X. Wang, et al. 2023. "The Phased Telomere-To-Telomere Reference Genome of *Musa acuminata*, a Main Contributor to Banana Cultivars." *Scientific Data* 10: 631.
- Liu, Z., M. Zhao, and J. Li. 2022. "Aroma Volatiles in Litchi Fruit: A Mini-Review." *Horticulturae* 8: 1166.
- Lu, X., P. Lü, H. Liu, et al. 2022. "Identification of Chilling Accumulation-Associated Genes for Litchi Flowering by Transcriptome-Based Genome-Wide Association Studies." *Frontiers in Plant Science* 13: 819188.
- Ma, M.-M., H.-F. Zhang, Q. Tian, et al. 2024. "MIKC Type MADS-Box Transcription Factor LcSVP2 Is Involved in Dormancy Regulation of the Terminal Buds in Evergreen Perennial Litchi (*Litchi chinensis* Sonn.)." *Horticulture Research* 11: uhae150.
- Maccaferri, M., M. Bruschi, and R. Tuberosa. 2022. "Sequence-Based Marker Assisted Selection in Wheat." In *Wheat Improvement: Food Security in a Changing Climate*, 513–538. Springer International Publishing.
- Machanick, P., and T. L. Bailey. 2011. "MEME-ChIP: Motif Analysis of Large DNA Datasets." *Bioinformatics* 27: 1696–1697.
- McGrath, K. C., B. Dombrecht, J. M. Manners, et al. 2005. "Repressorand Activator-Type Ethylene Response Factors Functioning in Jasmonate Signaling and Disease Resistance Identified via a Genome-Wide Screen of *Arabidopsis* Transcription Factor Gene Expression." *Plant Physiology* 139: 949–959.
- McKenna, A., M. Hanna, E. Banks, et al. 2010. "The Genome Analysis Toolkit: A MapReduce Framework for Analyzing Next-Generation DNA Sequencing Data." *Genome Research* 20: 1297–1303.
- Nakano, T., K. Suzuki, T. Fujimura, and H. Shinshi. 2006. "Genome-Wide Analysis of the ERF Gene Family in *Arabidopsis* and Rice." *Plant Physiology* 140: 411–432.
- Nguyen, L.-T., H. A. Schmidt, A. Von Haeseler, and B. Q. Minh. 2015. "IQ-TREE: A Fast and Effective Stochastic Algorithm for Estimating Maximum-Likelihood Phylogenies." *Molecular Biology and Evolution* 32: 268–274.
- Ohto, M.-A., S. K. Floyd, R. L. Fischer, R. B. Goldberg, and J. J. Harada. 2009. "Effects of APETALA2 on Embryo, Endosperm, and Seed Coat Development Determine Seed Size in *Arabidopsis*." *Sexual Plant Reproduction* 22: 277–289.
- O'Malley, R. C., S.-S. C. Huang, L. Song, et al. 2016. "Cistrome and Epicistrome Features Shape the Regulatory DNA Landscape." *Cell* 165: 1280–1292.
- Ou, J., S. A. Wolfe, M. H. Brodsky, and L. J. Zhu. 2018. "Motifstack for the Analysis of Transcription Factor Binding Site Evolution." $Nature\ Methods\ 15:8-9.$
- Pan, X., X. Lu, L. Huang, et al. 2025. "Histone Modification H3K27me3 Is Essential During Chilling-Induced Flowering in *Litchi chinensis*." *Plant Physiology* 197: kiae619.
- Pertea, M., G. M. Pertea, C. M. Antonescu, T.-C. Chang, J. T. Mendell, and S. L. Salzberg. 2015. "StringTie Enables Improved Reconstruction of a Transcriptome From RNA-Seq Reads." *Nature Biotechnology* 33: 290–295.
- Ramírez, F., F. Dündar, S. Diehl, B. A. Grüning, and T. Manke. 2014. "DeepTools: A Flexible Platform for Exploring Deep-Sequencing Data." *Nucleic Acids Research* 42: W187–W191.
- Rana, M. M., T. Takamatsu, M. Baslam, et al. 2019. "Salt Tolerance Improvement in Rice Through Efficient SNP Marker-Assisted Selection Coupled With Speed-Breeding." *International Journal of Molecular Sciences* 20: 2585.

- Rashotte, A. M., M. G. Mason, C. E. Hutchison, F. J. Ferreira, G. E. Schaller, and J. J. Kieber. 2006. "A Subset of *Arabidopsis* AP2 Transcription Factors Mediates Cytokinin Responses in Concert With a Two-Component Pathway." *Proceedings of the National Academy of Sciences* 103: 11081–11085.
- Rehman, S., and T. Mahmood. 2015. "Functional Role of DREB and ERF Transcription Factors: Regulating Stress-Responsive Network in Plants." *Acta Physiologiae Plantarum* 37: 1–14.
- Riechmann, J. L., and O. J. Ratcliffe. 2000. "A Genomic Perspective on Plant Transcription Factors." *Current Opinion in Plant Biology* 3: 423–434.
- Sakuma, Y., Q. Liu, J. G. Dubouzet, H. Abe, K. Shinozaki, and K. Yamaguchi-Shinozaki. 2002. "DNA-Binding Specificity of the ERF/AP2 Domain of *Arabidopsis* DREBs, Transcription Factors Involved in Dehydration- and Cold-Inducible Gene Expression." *Biochemical and Biophysical Research Communications* 290: 998–1009.
- Shen, S.-L., X.-R. Yin, B. Zhang, et al. 2016. "CitAP2.10 Activation of the Terpene Synthase CsTPS1 Is Associated With the Synthesis of (+)-Valencene in 'Newhall' Orange." *Journal of Experimental Botany* 67: 4105–4115.
- Shoji, T., M. Mishima, and T. Hashimoto. 2013. "Divergent DNA-Binding Specificities of a Group of Ethylene Response Factor Transcription Factors Involved in Plant Defense." *Plant Physiology* 162: 977–990.
- Słomka, M., M. Sobalska-Kwapis, M. Wachulec, G. Bartosz, and D. Strapagiel. 2017. "High Resolution Melting (HRM) for High-Throughput Genotyping—Limitations and Caveats in Practical Case Studies." *International Journal of Molecular Sciences* 18: 2316.
- Song, J., R. Liu, G. Chen, et al. 2023. "Two APETALA2/Ethylene Response Factors Coordinately With CaMYC2 Positively Regulate Capsaicinoid Biosynthesis in Pepper (*Capsicum annuum*)." *Horticultural Plant Journal* 11: 275–289.
- Song, L., R. Wang, X. Yang, A. Zhang, and D. Liu. 2023. "Molecular Markers and Their Applications in Marker-Assisted Selection (MAS) in Bread Wheat (*Triticum aestivum* L.)." *Agriculture* 13: 642.
- Sun, P., R. C. Schuurink, J.-C. Caissard, P. Hugueney, and S. Baudino. 2016. "My Way: Noncanonical Biosynthesis Pathways for Plant Volatiles." *Trends in Plant Science* 21: 884–894.
- Sun, Q., Z. He, D. Feng, et al. 2024. "The Abscisic Acid-Responsive Transcriptional Regulatory Module CsERF110-CsERF53 Orchestrates Citrus Fruit Coloration." *Plant Communications* 5: 101065.
- Sun, X., C. Jiao, H. Schwaninger, et al. 2020. "Phased Diploid Genome Assemblies and Pan-Genomes Provide Insights Into the Genetic History of Apple Domestication." *Nature Genetics* 52: 1423–1432.
- Tang, W., J. Lin, Y. Wang, et al. 2022. "Selection and Validation of 48 KASP Markers for Variety Identification and Breeding Guidance in Conventional and Hybrid Rice (*Oryza sativa* L.)." *Rice* 15: 48.
- UniProt Consortium. 2019. "UniProt: A Worldwide Hub of Protein Knowledge." *Nucleic Acids Research* 47: D506–D515.
- Upadhyay, R. K., D. K. Soni, R. Singh, et al. 2013. "SIERF36, an EAR-Motif-Containing ERF Gene From Tomato, Alters Stomatal Density and Modulates Photosynthesis and Growth." *Journal of Experimental Botany* 64: 3237–3247.
- von Maydell, D. 2023. "PCR Allele Competitive Extension (PACE)." In *Plant Genotyping: Methods and Protocols*, 263–271. Springer.
- Wang, Q., H. Liu, M. Zhang, S. Liu, Y. Hao, and Y. Zhang. 2020. "MdMYC2 and MdERF3 Positively Co-Regulate α-Farnesene Biosynthesis in Apple." *Frontiers in Plant Science* 11: 512844.

Waterhouse, A. M., J. B. Procter, D. M. Martin, M. Clamp, and G. J. Barton. 2009. "Jalview Version 2—A Multiple Sequence Alignment Editor and Analysis Workbench." *Bioinformatics* 25: 1189–1191.

Wei, C., M. Li, X. Cao, et al. 2022. "Linalool Synthesis Related PpTPS1 and PpTPS3 Are Activated by Transcription Factor PpERF61 Whose Expression Is Associated With DNA Methylation During Peach Fruit Ripening." *Plant Science* 317: 111200.

Wei, S., X. Li, Z. Lu, et al. 2022. "A Transcriptional Regulator That Boosts Grain Yields and Shortens the Growth Duration of Rice." *Science* 377: eabi8455.

Wu, B., X. Cao, H. Liu, et al. 2019. "UDP-Glucosyltransferase PpUGT85A2 Controls Volatile Glycosylation in Peach." *Journal of Experimental Botany* 70: 925–936.

Wu, Y., X. Li, J. Zhang, et al. 2022. "ERF Subfamily Transcription Factors and Their Function in Plant Responses to Abiotic Stresses." *Frontiers in Plant Science* 13: 1042084.

Xie, J., Y. Chen, G. Cai, R. Cai, Z. Hu, and H. Wang. 2023. "Tree Visualization by One Table (tvBOT): A Web Application for Visualizing, Modifying and Annotating Phylogenetic Trees." *Nucleic Acids Research* 51: W587–W592.

Yamasaki, K., T. Kigawa, M. Seki, K. Shinozaki, and S. Yokoyama. 2013. "DNA-Binding Domains of Plant-Specific Transcription Factors: Structure, Function, and Evolution." *Trends in Plant Science* 18: 267–276.

Yasui, Y., and T. Kohchi. 2014. "Vascular Plant One-Zinc FINGER1 and VOZ2 Repress the Flowering Locus C Clade Members to Control Flowering Time in Arabidopsis." Bioscience, Biotechnology, and Biochemistry 78: 1850–1855.

Yasui, Y., K. Mukougawa, M. Uemoto, et al. 2012. "The Phytochrome-Interacting Vascular Plant One–Zinc Finger1 and VOZ2 Redundantly Regulate Flowering in *Arabidopsis*." *Plant Cell* 24: 3248–3263.

Yauk, Y. K., C. Ged, M. Y. Wang, et al. 2014. "Manipulation of Flavour and Aroma Compound Sequestration and Release Using a Glycosyltransferase With Specificity for Terpene Alcohols." *Plant Journal* 80: 317–330.

Yuste-Lisbona, F. J., A. Fernández-Lozano, B. Pineda, et al. 2020. "ENO Regulates Tomato Fruit Size Through the Floral Meristem Development Network." *Proceedings of the National Academy of Sciences of the United States of America* 117: 8187–8195.

Zeng, R., Y. Shi, L. Guo, et al. 2025. "A Natural Variant of *COOL1* Gene Enhances Cold Tolerance for High-Latitude Adaptation in Maize." *Cell* 188: 1315–1329.e13.

Zhang, L., L. Chen, S. Pang, et al. 2022. "Function Analysis of the ERF and DREB Subfamilies in Tomato Fruit Development and Ripening." *Frontiers in Plant Science* 13: 849048.

Zhang, X., L. Yu, M. Zhang, et al. 2024. "MdWER Interacts With MdERF109 and MdJAZ2 to Mediate Methyl Jasmonate- and Light-Induced Anthocyanin Biosynthesis in Apple Fruit." *Plant Journal* 118: 1327–1342.

Zhang, Y., T. Liu, C. A. Meyer, et al. 2008. "Model-Based Analysis of ChIP-Seq (MACS)." *Genome Biology* 9: 1–9.

Zhang, Y., Z. Zeng, H. Hu, et al. 2024. "MicroRNA482/2118 Is Lineage-Specifically Involved in Gibberellin Signalling via the Regulation of *GID1* Expression by Targeting Noncoding PHAS Genes and Subsequently Instigated phasiRNAs." *Plant Biotechnology Journal* 22: 819–832.

Zhuang, M., C. Li, J. Wang, et al. 2021. "The Wheat *SHORT ROOT LENGTH 1* Gene *TaSRL1* Controls Root Length in an Auxin-Dependent Pathway." *Journal of Experimental Botany* 72: 6977–6989.

Zhuo, M.-G., T.-Y. Wang, X.-M. Huang, et al. 2024. "ERF Transcription Factors Govern Anthocyanin Biosynthesis in Litchi Pericarp by

Modulating the Expression of Anthocyanin Biosynthesis Genes." *Scientia Horticulturae* 337: 113464.

Supporting Information

Additional supporting information can be found online in the Supporting Information section. Figure S1: Protein sequence and folding models analysis of DREB/ERFs. Figure S2: Phylogenetic analysis and expression profiles of DREB/ERFs in five organs of lychee. a, Phylogenetic tree of the DREB/ERF gene family in lychee. 45 members marked with red dots have undergone DAP-seq analysis, and another ten members marked with grey dots have been selected but failed for DAP-seq analysis due to experimental constraints. The red and blue blocks represent the DREB and ERF subfamilies, respectively. The numbers next to the branches of the phylogenetic tree indicate bootstrap values. Gene IDs label the leaves of the phylogenetic tree, where DREB/ERF genes with 'm,' 'a,' or 'b' at the end have been manually corrected for structural annotation. Specifically, 'm' indicates errors or omissions in the original structural annotations, while 'a' and 'b' denote tandem duplicates that were incorrectly annotated as a single gene. b, Expression pattern of DREB/ERFs in five organs (leaves, carpel and stamen of different sexual types of lychee flower, seed, pericarp and aril) of lychee. Figure S3: Binding events of 45 DREB/ERFs undergone DAP-seq analysis. Figure S4: Top motif identified for each DREB/ERF member based on all peaks associated with each member. Figure S5: Correlation of binding events of DREB/ERFs among the ten groups. Figure S6: Expression pattern of DREB/ERFs in five organs of lychee. Figure S7: Number of genes that were bound by six key DREB/ERFs and co-expressed with them. Figure S8: The DNA-binding events in the first exon of three tandemly repeated *LcTPS*s. **Figure S9:** Sequence analysis of three *LcTPS*s. Figure S10: PAGE electrophoresis image of GST-LITCHI017494-cut protein. Figure S11: Binding events of DREB/ERFs in two haplotypes of lychee. Figure S12: Functional validation of LcSVP in Arabidopsis. Figure S13: Protein sequence and folding models analysis of DREB/ ERFs in *Arabidopsis*. **Table S1:** List of *DREB/ERFs* in lychee. **Table S2:** Primers for LcDREB/ERFs amplification. Table S3: Primers for EMSA, Y1H, DLR, subcellular localization, construction and confirmation of transient expression in N. benthamiana. Table S4: List of lychee resequencing samples used in this study.